

Plastic Deformation and failure studies near a void for Copper-Aluminium alloy via Molecular Dynamics Simulation

A thesis submitted in partial fulfillment of the requirements for the degree of

Bachelor of Technology

In

Metallurgical and Materials Engineering

By

**Ashis Das (110MM0261)
Gaurav Singh (110MM0553)**

Under the supervision of

Prof. NATRAJ YEDLA



Department of Metallurgical and Materials Engineering
National Institute of Technology, Rourkela
2014

National Institute of Technology, Rourkela

CERTIFICATE

This is to certify that the thesis entitled “**Plastic Deformation and failure studies near a void for Copper-Aluminium alloy via Molecular Dynamics Simulation**” submitted by Ashis Das, Roll No. 110MM0261 and Gaurav Singh Roll No. 110MM0553 in partial fulfillment of the requirements for the award of Bachelor of Technology degree in Metallurgical and Materials Engineering at the National Institute of Technology, Rourkela (Deemed University) is an authentic work carried out by them under my supervision and guidance. To the best of my knowledge, the matter embodied in the thesis has not been submitted to any other University/Institute for the award of any Degree or Diploma.

DATE :- 8/05/2014

Prof:- NATRAJ YEDLA

Department of Metallurgical and Materials Engineering

ACKNOWLEDGEMENT

This project would not have been possible without the help, support, and cooperation of many. At the outset, we would like to express our sincere gratitude to our supervisor Prof. Natraj Yedla for his invaluable guidance and support at all times and his guidance throughout the duration of the project. We would also like to extend our indebtedness to Prof. Natraj Yedla for his valuable guidance, constant encouragement and kind help and advice at various stages during the execution of this work. His encouragement and comments kept our endeavors alive, and helped us to establish the overall direction of the project.

We would also like to express our gratitude to Prof. B.C.Ray, Head of the Department, Metallurgical and Materials Engineering for allowing us access to the laboratory facilities in the department.

Our sincere thanks to family and friends who have provided us with inspirational words, a welcome ear, new ideas, and their invaluable time.

Ashis Das
Roll no: 110MM0261

Gaurav Singh
Roll no: 110MM0553

Department of Metallurgical and Materials Engineering,
National Institute Of Technology, Rourkela
Rourkela-769008

ABSTRACT

Molecular Dynamics (MD) simulations of uniaxial as well as for biaxial tension at nano-scale was carried out for different strain rates and at different temperatures on $\text{Cu}_{50}\text{Al}_{50}$ alloy specimen having a void in order to investigate the nature of deformation as well as fracture near the void. It was seen that failure occurred in a similar manner to what is observed at macro scale i.e. by several voids formation, coalescence of void these voids into cracks leading to failure of the specimen. The engineering Stress-Strain diagram observed for the specimen showed a series of fluctuations in the stress value. The first drop in the stress can be attributed to the yielding of the material and subsequent drops could be due to formation of new voids. In most of the cases the specimen fractured by multiple necking. In case of deformation by biaxial mode no distinct trend is observed. The specimen fractured at various points unlike in case of uniaxial loading.

Table of Contents

1.1 Introduction to Copper-Aluminium alloys	9
2 . <i>Procedure of MD Simulation</i>	10
2 Introduction to Modeling and Simulations	11
2.1 Model:	11
2.3 Molecular Dynamics Simulation	11
2.3.1 Introduction:.....	11
2.4 Design Parameters in MD Simulation:	13
2.4.1 Micro-canonical or NVE ensemble:	13
2.4.2 Canonical or NVT ensemble:.....	13
2.4.3 Isothermal–Isobaric or NPT ensemble:.....	13
2.5 Empirical Potentials:	14
2.6 Pair wise and Many-Body Potentials:	14
2.7 Semi-Empirical Potentials:	14
2.8 Polarizable Potentials:.....	14
2.9 Ab-initio Quantum-Mechanical Methods:	14
2.10 Algorithms in Molecular Dynamics [6,7]:	15
2.11 Applications of MD simulation [5]:.....	16
2.12 LAMMPS & VMD [5,6, 9].....	16
2.13 Simulation Procedures	17
2.13.1 Procedures:.....	17
2.13.2 Output of Simulation:.....	17
3. Plastic Deformation of Metal Crystals.....	19
3.2 Deformation by slip	20
3.2.1 Slip Bands	21
3.2.2 Slip by dislocation motion	22
3.2.3 Critical resolved shear stress for slip [8].....	22
3.3 Deformation by twinning	23
4. <i>Results and Discussion</i>	25
4.1 Creation of Copper-Aluminium (Cu ₅₀ Al ₅₀) alloy and tensile deformation procedure	26
4.1.1 Sample preparation	26
4.2 Tensile Deformation of Alloy Specimen:	28

4.2.1 Computational Steps:	28
4.2.2 Uniaxial Testing of the specimen.....	28
4.3 Simulation results.....	30
4.4 Tensile testing at 10^{11} s^{-1} strain rate for different temperatures	30
4.4.1 Comparison of uniaxial-tensile properties of the specimen at different temperatures	30
4.5 Tensile testing $5 \times 10^{11} \text{ s}^{-1}$ strain rate for different temperatures.....	35
5 4.5.1 Comparison of Tensile properties of the specimen at different temperatures.....	35
4.6 Effect of varying temperature at 10^{12} strain rate	39
4.6.1 Comparison of Tensile properties of the specimen at different temperatures	39
5. Biaxial tensile testing of $\text{Cu}_{50}\text{Al}_{50}$ alloy at different strain rates.....	44
6. Conclusions	47
7. References	48

LIST OF FIGURES

Fig 4.1	Stress Strain curve for Cu ₅₀ Al ₅₀ Alloy at 10 ¹¹ Strain rate and at different temperatures (50K, 300K, 400K)
Fig 4.2	Fig 4.3 VMD snapshots of the specimen when deformed in elastic region at strain rate of 0.1 ps ⁻¹ applied in y direction
Fig 4.3	VMD snapshots of the specimen at different strain values
Fig 4.4	VMD snapshots of the specimen at the time of getting fractured
Fig 4.5	VMD snapshots depicting failure of the CU ₅₀ Al ₅₀ alloy when tensile testing is carried out at 300K
Fig 4.6	VMD snapshots depicting failure of the CU ₅₀ Al ₅₀ alloy when tensile testing is carried out at 500K
Fig 4.7	Stress Strain curve for Cu ₅₀ Al ₅₀ Alloy at 5 x10 ¹¹ Strain rate and at different temperatures (50K, 300K, 400K)
Fig 4.8	VMD snapshots depicting failure of the CU ₅₀ Al ₅₀ alloy when tensile testing is carried out at 50K (a)900; (b)1500; (c)2800; (d)3500; (e)4300; (f) 5000 timesteps
Fig 4.9	VMD snapshots depicting failure of the CU ₅₀ Al ₅₀ alloy when tensile testing is carried out at 50K (a)900; (b)1500; (c)2800; (d)3500; (e)4300; (f) 5000 timesteps
Fig 4.10	VMD snapshots depicting failure of the CU ₅₀ Al ₅₀ alloy when tensile testing is carried out at 50K (a)900; (b)1500; (c)2800; (d)3500; (e)4300; (f) 5000 timesteps
Fig 4.11	Stress Strain curve for Cu ₅₀ Al ₅₀ Alloy at 10 ¹² Strain rate and at different temperatures (50K, 300K, 400K)
Fig 4.12	VMD Snapshots of the rearrangement of atoms to form new crystal structure during tensile testing resulting in near closure of the voids
Fig 4.13	VMD snapshots showing the failure of the specimen via formation of

	new voids and their coalescence to form nano cracks
Fig 4.14	VMD snapshot showing failure of Cu ₅₀ Al ₅₀ alloy when tested at 10 ¹² s ⁻¹ strain rate for 300 at (a)100,(b)1000,(c)1500,(d)2000,(e)2500,(f)3000 timesteps
Fig 4.15	VMD snapshot showing failure of Cu ₅₀ Al ₅₀ alloy when tested at 10 ¹² s ⁻¹ strain rate at 400K (a)100,(b)1000,(c)1500,(d)2000,(e)2500,(f)3000 timesteps
Fig 5.1	Stress Strain curve for various strain rates under biaxial loading
Fig 5.2	VMD snapshot showing the failure of the specimen for 10 ¹¹ strain rate at 300K
Fig 5.3	VMD snapshot showing the failure of the specimen at 5x10 ¹¹ strain rate at 300K
Fig 5.4	VMD snapshots showing the failure of the specimen for 10 ¹² strain rate at 300K

1. Introduction

1.1 Introduction to Copper-Aluminium alloys

Copper-Aluminium alloys are also called Aluminium Bronzes. Varieties of Cu-Al alloys of different compositions have been utilized for industrial use. Cu-Al alloys are well known for their high strength and corrosion resistance as compared to other bronze alloys. These alloys are tarnish-resistant and show low rates of corrosion in atmospheric conditions, low oxidation rates at high temperatures, and low reactivity with sulfurous compounds and other exhaust products of combustion. They are also resistant to corrosion in sea water. Aluminium bronzes' resistance to corrosion rests in the aluminium component of the alloys, which reacts with atmospheric oxygen to form a thin, tough surface layer of alumina (aluminium oxide) which acts as a barrier to corrosion of the copper-rich alloy. The addition of tin can improve corrosion resistance [1].

Aluminum bronze alloys typically contain 9-12% aluminum and up to 6% iron and nickel. Alloys in these composition limits are hardened by a combination of solid solution strengthening, cold work, and precipitation of an iron rich phase. High aluminum alloys are quenched and tempered. Aluminum bronzes are used in marine hardware, shafts and pump and valve components for handling seawater; sour mine waters, non-oxidizing acids, and industrial process fluids. They are also used in applications such as heavy duty sleeve bearings, and machine tool ways. They are designated by UNS C60800 through C64210. Aluminum bronze castings have exceptional corrosion resistance, high strength, and toughness and wear resistance and good casting and welding characteristics. Aluminum bronze castings are designated as UNS C95200 to C95900. Aluminium bronzes are most commonly used in applications where their resistance to corrosion makes them preferable to other engineering materials. These applications include plain bearings and landing gear components on aircraft, engine components (especially for seagoing ships), underwater fastenings in naval architecture, and ship propellers. Aluminum bronze is also used to fulfill the ATEX directive for Zones 1, 2, 21, and 22. The attractive gold-toned coloration of aluminium bronzes has also led to their use in jewelry [2].

Aluminium bronzes are in the highest demand from the following industries and areas:

- General sea water-related service
- Water supply
- Oil and petrochemical industries (*i.e.* tools for use in non-sparking environments)
- Specialized anti-corrosive applications
- Certain structural retrofit building applications.

Aluminium bronze can be welded using the MIG welding technique with an aluminium bronze core and pure argon gas. Aluminium bronze is used to replace gold for the casting of dental crowns. The alloys used are chemically inert and have the appearance of gold. Since there are several applications of these alloys we need to understand the deformation behavior. So, classical molecular dynamics (MD) simulations were carried out to understand the deformation behavior at the atomic level. As most of these alloys are obtained by casting route there is possibility of presence of defects. The presence of defects such as voids at the nano-level and their effect on the mechanical properties is not clearly known. So in the present study we investigated the effect of strain rate, temperature, mode of deformation on the Cu₅₀Al₅₀ alloy 2D-model.

2 .Procedure of MD Simulation

2 Introduction to Modeling and Simulations

2.1 Model:

It can be simply defined as a simplified exhibition of a system at some particular instant of time or space, to promote understanding of the real life systems as its objective.

TYPES OF MODELS:

1. Atomistic Modeling
2. Monte Carlo
3. Continuum

Atomistic simulation models materials at the level of atoms using modern computing power

So as to include every atom in the model. Since interacting atoms are the foundation and base of materials science, atomistic modeling has helped a lot in the field of computational materials studies. It can be classified broadly into two categories

1. Molecular statics
2. Molecular Dynamics

In Molecular statics the relaxed configuration (positions and velocities) of atoms is found by conjugate gradient method or some similar energy minimization method. These simulations provide information of crystal lattice structure in different phases and under different conditions [3].

In case of Molecular Dynamics the actual motion of atoms is simulated by evolving the atomic configuration (atomic positions and velocities) with time by integrating Newton's Equation of Motion [3].

Force = mass x acceleration

2.3 Molecular Dynamics Simulation

2.3.1 Introduction:

Molecular dynamics (MD) method can reproduce the macro-properties of a material, and store a great deal of valuable micro-information. Therefore, it was considered as an important tool to associate with the macro-scale and micro-scale [4]. Molecular dynamics (MD) is a computer simulation technique where the time evolution of a set of interacting atoms and molecules of a system is followed by integrating their equations of motion ($F=ma$). The atoms and molecules present in the system are allowed to interact for a period of time. The trajectories obtained of the interacting particles are determined by numerically solving Newton's equations of motion where forces between the particles and potential energy are defined by molecular mechanics force fields. The Newton's equation of motion can be expressed mathematically as follows:

$$F = m_i a_i \dots\dots\dots (i)$$

$$a_i = d^2 r_i / dt^2 \dots\dots\dots (ii)$$

Where F = interatomic force between the interacting particles

m_i = mass of each particle (considering a homogeneous system, mass

of each particle is same)

a_i = Acceleration of each particle

r_i = particle position

If given an initial set of positions as well as velocities, the subsequent time evolution through which the particle interaction and movement takes place can be completely determined. During Simulation process atoms and molecules will move inside the computer, bumping into each other during the interactions, if constrained vibrating about a mean position, or may be wandering around (if the system is fluid), oscillating in waves in concert with their neighbors, or may be evaporating away from the system if there is a free surface involved, and so on, in a way similar to what real atoms and as well as molecules would do in real life.

The initialization of MD Simulation begins with initializing the position and velocities of atoms and after that by calculating the total energy which includes bond energy, torsional energy, bond angle energy, as well as non-bond energy. Then after that the forces on the atoms are calculated. Subsequently the atoms are moved and to obtain the atomic trajectory newton's equation of motion is integrated.

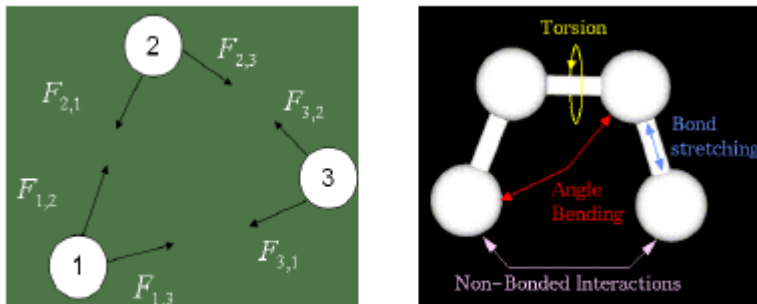


Fig 3.2 Figure showing various forces of interaction between atoms.

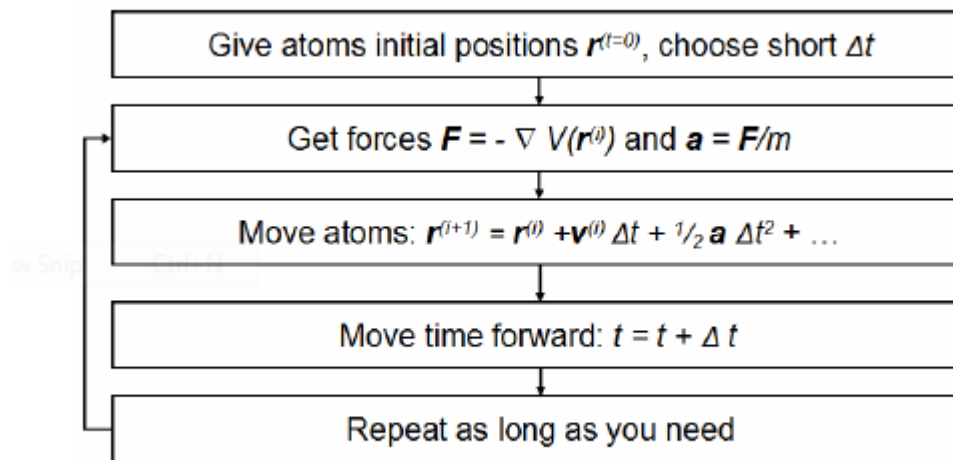


Fig 3.3. The process algorithm for Molecular Dynamics simulation [5]

Since any molecular system contains of a very large no of micro-particles, atoms or molecules, it is quite impractical and most of the times impossible to characterize the properties of such a vast system analytically. In these cases MD simulation comes handy to solve these problems by using numerical methods. To achieve the simulation results that are error free, calculations are made algorithms are written in a proper manner which is then implemented on a programming language easy to operate. Due to its important commercial applications in large scale, this kind of simulation technique is now gaining much more popularity.

2.4 Design Parameters in MD Simulation:

The study on the dynamics of large macro-molecules along with the optimization of resulting structures is facilitated by MD simulation. As discussed earlier the trajectory obtained by molecular dynamics as per the algorithm provided gives a set of conformations of molecule. As the simulation progresses with atomic movements, thermodynamic parameters of the system like temperature, total energy, pressure, volume gets modified and finally we get the desired result based on the algorithm used. Depending on these parameters, simulation can be done in various ways. They are as follows [6, 7]:

2.4.1 Micro-canonical or NVE ensemble:

Here the system is restrained from changes in moles (N), volume (V) and energy (E). It corresponds to an adiabatic process i.e. no heat exchange. A micro-canonical molecular dynamics trajectory may be measured as an exchange of potential energy and kinetic energy and where the total energy is being conserved [6].

2.4.2 Canonical or NVT ensemble:

In this case, moles (N), volume (V) and temperature (T) are conserved in the system. Therefore NVT ensemble is sometimes also called constant temperature molecular dynamics (CTMD). In NVT, the energy of endothermic and exothermic processes is exchanged with a thermostat. To add and remove energy from the boundaries of an MD system in a more or less actual way, approximately defining the canonical ensemble, a variety of thermostat methods is available.[6].

2.4.3 Isothermal–Isobaric or NPT ensemble:

In this case also, moles (N), pressure (P) and temperature (T) are conserved. With a thermostat sometimes a barostat is needed to control the pressure to approximate real situation. In accordance with available computational power the design of a molecular dynamics simulation should be made. Various parameters like simulation size (n=number of particles), timestep and total time for simulation must be selected carefully so that the calculation can be completed within a reasonable time period [6].

Multiple factors affect the total simulation time and they should be taken into consideration. In the case of a classical MD simulation, the most important task of CPU is the evaluation of the potential (force field) as a function of the particles' internal coordinates.

Calculations are more time-consuming, while encountering the non-bonded or non-covalent parts of a system. Potential function or force field measures quantitatively how the particles will interact and represent a classical treatment of particle-particle interactions that results in structural and conformational changes but usually cannot reproduce chemical reactions. Various

potentials that are widely used in simulation are given below and choice of potential depends on the user depending on the type of material system we are dealing with.

2.5 Empirical Potentials:

Those used in chemistry are frequently called force fields, but material physics gives it a different name. Most force fields in chemistry are empirical. They consist of a summation of bonded forces associated with chemical bonds, forces due to bond angles, torsional forces and non-bonded forces associated with Vander Waals forces and electrostatic charge. The total potential energy can be expressed as:

$$E_{\text{pot}} = \sum V_{\text{bond}} + \sum V_{\text{ang}} + \sum V_{\text{torsion}} + \sum V_{\text{vdW}} + \sum V_{\text{ele}} + \dots$$

This is the main reason of MD simulations being slow.

2.6 Pair wise and Many-Body Potentials:

The total potential energy is calculated from the sum of energy contributions between an atomic pair in pair wise potentials. To illustrate, an example of such a pair potential is the non-bonded Lennard–Jones potential used for calculating Van der Waals forces. The potential energy includes the effects of three or more particles interacting among themselves in many-body potentials. In simulations with pairwise potentials, a global contact exists in the system, but they occur only through pairwise terms. Whereas in the case of many-body potentials, it is difficult to get the potential energy by a sum over pairs of atoms because these calculations are done explicitly as a combination of higher-order terms. For example, the Tersoff potential and the most widely used embedded-atom method (EAM).

2.7 Semi-Empirical Potentials:

Semi-Empirical Potentials makes use of the matrix representation from quantum mechanics. The matrix is then diagonalized to determine the occupancy of the different atomic orbitals, and empirical formulae are used to determine the energy contributions of the orbitals.

2.8 Polarizable Potentials:

It includes the effect of polarizability. It means that by calculating the partial charges obtained from quantum chemical calculations. It allows for a redistribution of charge between atoms responding to the local chemical environment. To obtain better simulation results for systems like water and protein, polarizability can be introduced.

2.9 Ab-initio Quantum-Mechanical Methods:

The amount of information Ab-initio calculations produce can't be obtained from empirical methods. Factors like density of electronic states or other electronic properties can't be obtained from empirical methods. On the contrary, the unique advantage of using ab-initio methods is the ability to study reactions that involve breaking or formation of covalent bonds, which correspond

to multiple electronic states. The size of the timestep required for integration which is same as the time length between evaluations of the potential function is another factor that affects total CPU time required by a simulation.

The time step must be chosen small enough to avoid discretization errors. Typical time steps used for classical MD are in the order of 1 femtosecond (10⁻¹⁵ s). To achieve optimum simulation time, proper time integration algorithm should be implemented.

2.10 Algorithms in Molecular Dynamics [6,7]:

The engine of a molecular dynamics program is its time integration algorithm. Time integration algorithms are based on finite difference principles, which involve discretization of on a finite grid, the time step Δt being the distance between consecutive points. Finding the positions and some of their time derivatives at an instant t , the integration scheme gives the same quantities at a later time $t+\Delta t$. By iterating the procedure, the time evolution of the system can be followed for long times. The schemes are approximate and there are errors associated with them which can be reduced by decreasing Δt .

Two popular integration methods for MD calculations are the Verlet algorithm and predictor corrector algorithms. Out of these two Verlet algorithm is mostly used. In this case, the position of a particle at any time t is given by:

$$V(t) = \{r(t+\Delta t) - r(t-\Delta t)\} / \{2\Delta t\} \dots\dots\dots (iii)$$

Where $V(t)$ = Velocity of a particle at time t .

$R(t)$ = position of a particle at time t .

Δt = Small change in time.

The predictor-corrector algorithm comprises of three steps

- Step 1: Predictor: From the positions and their time derivatives at time t , one ‘predicts’ the same quantities at time $t+\Delta t$ by means of a Taylor expansion. One such quantity is acceleration
- Step 2: Force evaluation: The force is computed by taking the gradient of the potential at specified locations. The deviation between the resulting acceleration and the predicted acceleration gives error.
- Step 3: Corrector. This error signal is used to ‘correct’ positions and their relative derivatives.

The simulation box size must be sufficient enough to avoid surface defects in all kinds of molecular dynamics simulations. Boundary atoms have fewer neighbors than atoms inside resulting surface. This effect in the simulation to be much more important than they are in the real system. Most of the time Boundary conditions treated by choosing fixed values at the edges, or by the process of employing periodic boundary conditions where the particles interact across the boundary and can move from one end to another end.

2.11 Applications of MD simulation [5]:

- For simulation and study of bio-molecular systems like protein synthesis and characterization.
- Designing of drugs in pharmaceutical industry to test properties of a molecule without even synthesizing it.
- Study of the effect of particles like neutrons and ion irradiation on solid surfaces.
- It has wide range of applications in materials sectors too where experiments relating any problem are very difficult to perform in laboratory conditions.
- It is also used to study various kind of properties of metals, non-metals and alloys like fatigue properties, tensile properties, deformation behavior, high temperature behavior etc.

2.12 LAMMPS & VMD [5,6, 9]

- LAMMPS is an acronym for Large-scale Atomic/Molecular Massively Parallel Simulator. This is the basic code required to do materials simulation.
- LAMMPS consists of potentials for soft materials and solid-state materials and many more kinds of materials.
- LAMMPS can be used to model atoms or as a parallel particle simulator at the atomic, meso, or continuum scale.
- LAMMPS makes use of MPI(Message Passing Interface) for parallel communication and is free, open-source software, distributed under the terms of the GNU General Public License[6].
- For computational efficiency LAMMPS uses neighbor lists to keep track of particles present at nearby location. The lists are optimized for systems with particles that are repulsive at small distances, resulting the local density of particles never becomes too large [5]. The code are written with the help of C++. The designing structure of the code is so flexible that it can be easily modified and extended with new applications.
- A combination of pre and post-processing tools are also packaged with LAMMPS, some of which can convert input and output files to/from formats used by other codes.
- VMD is a molecular visualization/graphics program designed for the display and analysis of molecular assemblies.
- VMD can simultaneously and spontaneously display any number of structures using a wide variety of rendering styles and coloring method [6].
- VMD provides a complete graphical user oriented interface for program control, as well as a text interface using the Tcl embeddable parser to allow for complex scripts with variable substitution, control loops and function calls [9].
- It is an open source code.
- In this project work, all the simulations were performed using LAMMPS software and resulting models and structures obtained by that were analyzed and using VMD visualization program.

2.13 Simulation Procedures

2.13.1 Procedures:

- First task in order to draw a simulation is to download LAMMPS software to our personal computer or laptop, which is itself a free source and is easily available on Sandia National Laboratories website.
- Three basic files or components are always required for running any simulation. They are as follows:
 - a) In file (program file to create models and performing simulation)
 - b) Potential file (contains data about inter atomic bond energy and force field between atoms)
 - c) Executable file (Imp_win_no-mpi.exe, required to run the commands in the in file).
- The next step is to open command prompt screen (dos environment) by typing “cmd” in address bar or in start icon.
- Then the screen will display the path address in which all the aforementioned files are present.
- After that next to the path address type Imp_win_no-mpi.exe< in file name then press enter.
- Then automatically the in file will be executed by the .exe file and if there is any error in the in file then it will be displayed in the command prompt screen and subsequent rectification will be required.

2.1.3.2 Output of Simulation:

- After successful running of the in file, we will get three out-put files as follows:
 - a) DUMP file (containing the atomic co-ordinates of the final structure after simulation and also for deformation studies it contains the stress component values)
 - b) Log file (containing thermodynamic data e.g. temperature, pressure, volume, and total energy after a particular no of steps)
 - c) Log. lammps file
- Now to see the final structure of our experimented sample after simulation, we have to open dump file containing atomic co-ordinates, through VMD software which need to be installed in the system separately.
- VMD has three parts.
 - a) VMD Main
 - b) Display Screen
 - c) Program Screen
- Necessary required adjustments to the finally achieved structure like change of color, display format (Atomic or point etc.), graphics representation styles can be done VMD main. In display screen we see the image of the final structure. In the program screen, any changes that we do in VMD main and final results are displayed accordingly.

3. Literature review

3. Plastic Deformation of Metal Crystals

Deformation occurs when a metal piece is subjected to uniaxial force

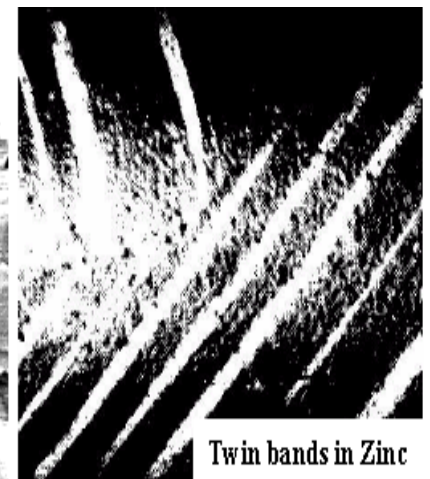
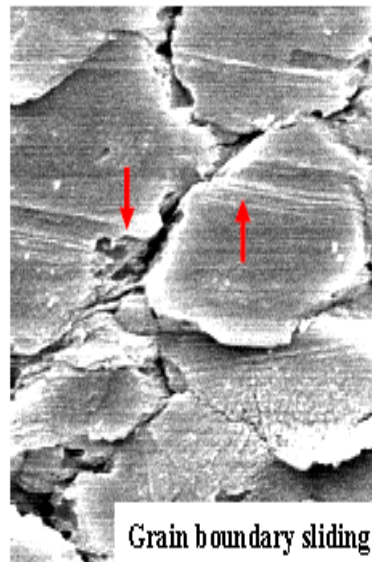
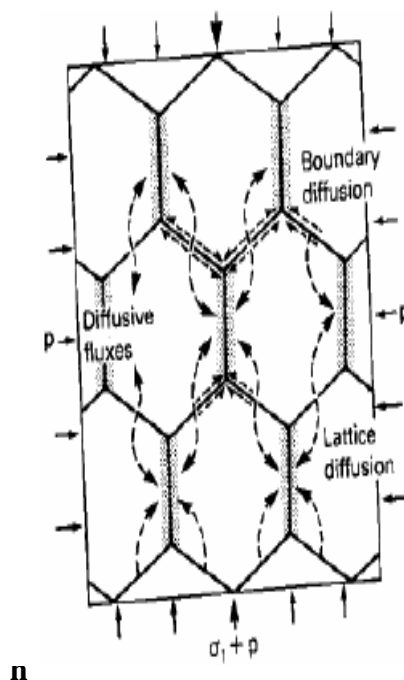
- When the force is removed: there may be 2 possibilities

The dimensions of the metal piece is restored because the atoms move to their original position called elastic deformation.

The atoms get replaced from their position to such an extent that the original shape of the metal piece could not be restored called plastic deformation.

Plastic deformation may take place:

- Slip
- Twinning
- Grain boundary sliding
- Diffusional creep
- Phase transformation



info.lu.farmingdale.edu/depts/

met/met205/image257.gif

owing different deformation mechanisms [8].

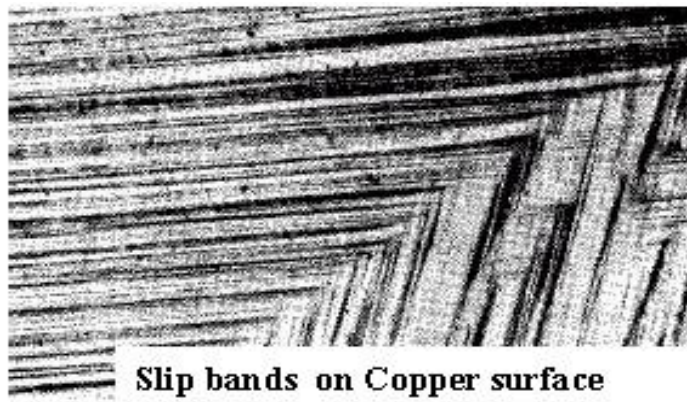


Fig 3.2 Showing slip bands on copper surface [8].

Two prominent mechanisms of plastic deformation, namely slip and twinning .

3.2 Deformation by slip

Plastic deformation in metals is generally produced by movement of dislocations or slips, which can be considered analogous to the real life example of the distortion produced in a deck of cards. Slip occurs only when the shear stress exceeds a critical value [8]. The atoms move certain atomic distances along the slip plane which is readily visible as the slip lines on the metal surface.

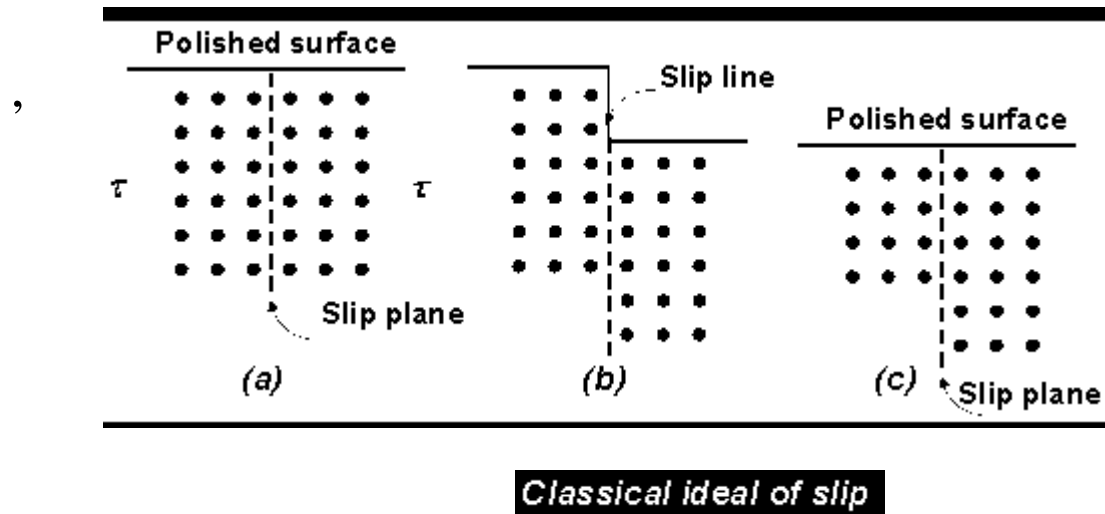


Fig 3.3 Showing an ideal slip [8].

3.2.1 Slip Bands

When the crystal structure is seen at higher magnifications discrete slip lamellae can be found. Slip is known to occur on certain crystallographic planes or the planes of greatest atomic density and in closed packed direction.

Slip planes in different crystal structures

BCC structure: $\{110\}$, $\{112\}$, $\{123\}$ planes and always in $\langle 111 \rangle$ direction

FCC structure: $\{111\}$ plane and in $\langle 110 \rangle$ direction.

HCP structure: (0001) basal plane and in $\langle 1120 \rangle$ direction

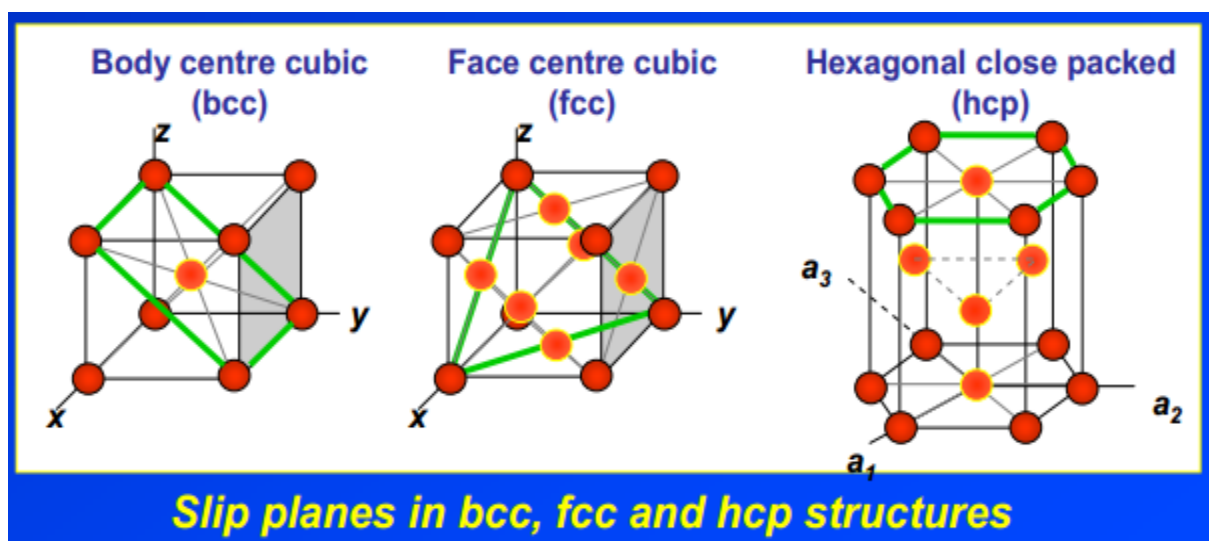
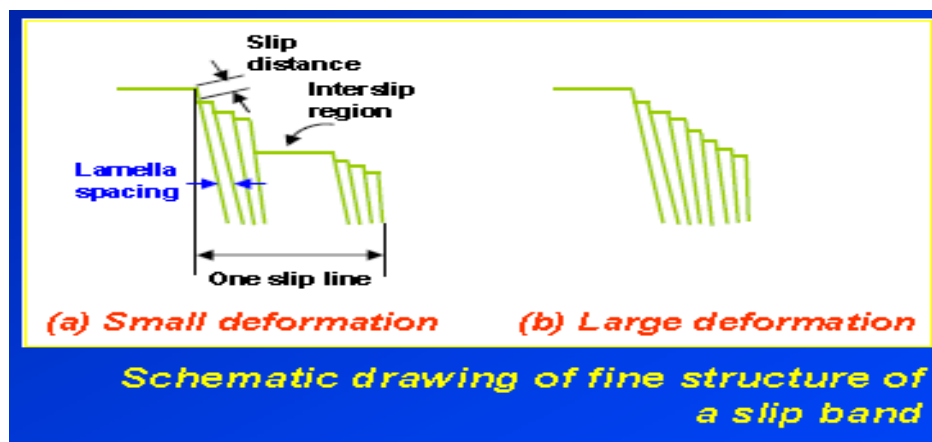


Fig 3.4 Showing slip planes in BCC, FCC and HCP crystals [8].

3.2.2 Slip by dislocation motion

Slip is a process of plastic deformation process which can also be produced by dislocation motion.

- Dislocation motion can be thought of analogous to the caterpillar movement model in real life.
- The caterpillar during its motion forms a hump with its position and its movement corresponds to that of the extra-half plane in the dislocation movement

3.2.3 Critical resolved shear stress for slip [8].

The extent of slip in a single crystal depends upon following factors:

1. The magnitude of the shear stress applied.
2. Crystal structure geometry.
3. The number of active slip plane in the direction of the shear stress.

Slip occurs when the shearing stress on the slip plane in the slip direction reaches a critical resolved shear stress[8].

- Schmid calculated the critical resolved shear stress from a single crystal tested in tension.
- The area of the slip plane $A' = A/\cos\phi$.
- The force acting in the slip plane A' is $P\cos\lambda$.

The critical resolved shear stress is given by the formula:

$$\tau_R = \frac{P \cos \lambda}{A / \cos \phi} = \frac{P}{A} \cos \phi \cos \lambda$$

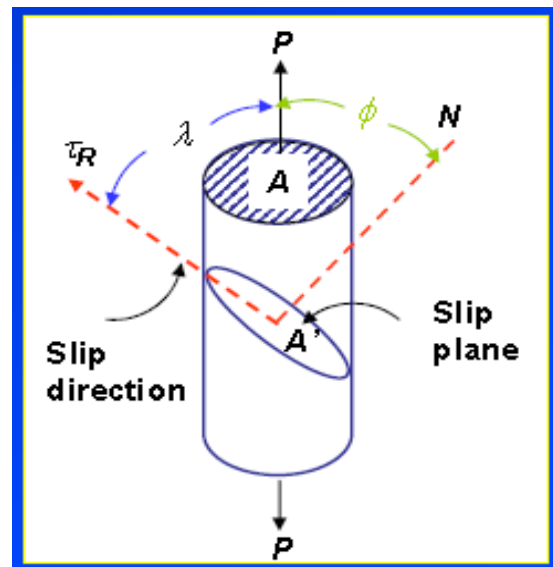


Fig 3.5 Calculation of CRSS [8].

3.3 Deformation by twinning

Twinning occurs in metallic crystals when one portion of the crystal takes up an orientation which is related to other portion in a definite symmetrical way [8]. The boundary which is the plane of symmetry between the two portions is called as twinning boundary. The essential condition for twinning is when the shear stress is greater than the critically resolved shear stress. Twinning occurs on a particular crystallographic plane and in a particular crystallographic direction.

Twin results from atomic displacement produced from

- 1) Applied mechanical shear force (mechanical twin) : in BCC, HCP
These are produced under the conditions of shock loading or rapid rate of loading and decreased temperatures. Twins are formed in very short span of time probably in few milliseconds.
- 2) During annealing heat treatment (annealing twin): in FCC

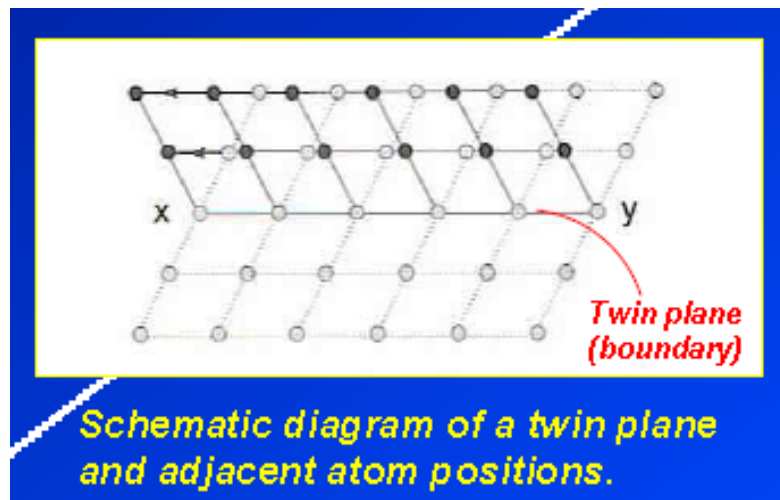


Fig 3.6 showing twin plane boundary [8].

R. Komanduri, N. Chandrasekaran, L.M. Raff [10]. studied Molecular Dynamics (MD) simulations of uniaxial tension at nanoscale which was carried out at constant rate of loading. The tests were carried out on some BCC as well as FCC crystal structure specimens in order to study the nature of deformation and also that of fracture. Failure of the specimens occurred during the process due to void formation, their coalescence into nanocracks, and subsequent fracture or separation were observed similar to what is observed at macroscale. A very characteristic feature of the engineering stress-strain plot was observed, rapid increase in the stress values then dropping to zero as the material failed via ductile fracture. With increasing deformation the neck's radius is found to increase and decrease as the ductility of the specimen decreases. In their investigation, they found out that the strain to fracture is less in case of BCC crystals than in case of FCC crystals. In case of BCC crystal system, stress-strain graph obtained didn't follow any linear trend. Instead, there seemed to be rapid rise and drop in the stress values on inspecting the graph. If the drop obtained in the stress strain curves can be attributed to the rearrangement of atoms to a new or modified crystalline structure, it appears that BCC materials undergo a significant change in their structure and subsequent realignment relative to the FCC materials [10].

Lin Yuan and Debin Shan, Bin Guo [11]. studied the MD simulation of tensile deformation of nano-single crystal aluminum. In order to find out the deformation process acting at nano scale MD simulation was done in order to simulate the tension process. The results showed a decrease in the stress value after linearly increasing to a maximum value. Thereafter multiple slips occur on the [111] plane after yielding. At last ductile fracture of the specimen occurs. The results obtained by the atomistic simulation of tension at nano scale is in accordance to the results obtained during tensile deformation at macro scale i.e. the tensile stress decreases on increasing temperature also lower yield stress is obtained at a lower strain rate value [11].

ZENG Xiang-guo, XU Shu-sheng, CHEN Hua-yan, and LI Ji-liang [12]. studied plastic deformation mechanism as well as failure near a void in a HCP crystal using VMD simulation. They used modified embedded atom method (MEAM) potentials in order to characterize the interactions between atoms of HCP crystal in this case magnesium alloy specimen with only a void. The results obtained by this study showed that the fracture mechanism near a void in magnesium alloy is a very complex process. Several factors are involved that lead to the growth of the void for e.g.: plastic blunting near the void, formation of micro-vacancies, coalescence of the voids all these factors lead to rapid crack growth. [12].

4. Results and Discussion

During the execution of this project work, the various simulations and analysis that have been carried out are as follows:

- Creation of Cu₅₀Al₅₀ alloy model consisting of a spherical void was made with the help of MD simulation.
- Study of various thermodynamic parameters during creation like Volume-temperature relation, temperature-time and structural characterization such as RDF plots.
- Uniaxial tensile as well as biaxial deformations of the Cu₅₀Al₅₀ specimens were carried out at various temperatures until fracture.
- Fracture behavior of Cu₅₀Al₅₀ alloy model containing the void was studied with the help of the simulation obtained.

4.1 Creation of Copper-Aluminium (Cu₅₀Al₅₀) alloy and tensile deformation procedure

Here purpose this simulation is to create a copper-aluminium crystalline 2D lattice with a fixed dimension of 100Å* 50Å *5 Å (length x width x thickness) with a cylindrical void in between having a radius of 5 Å at 50K and subsequently carrying out the tensile deformation of the created sample to obtain the stress-strain curves which will be used to explain the plastic deformation mechanism procedure near the void in the specimen. Given below is the infile which creates the Copper-Aluminium alloy consisting of 2317 atoms.

4.1.1 Sample preparation

This program is for obtaining 3d-crystal lattice

units	metal-> determines units of all quantities used in the input file
echo	both -> echoes each input script command to both log file and screen
atom_style	atomic
dimension	3
boundary	p p p -> periodic boundary condition
region	box block 0 50 0 100 0 5 units box -> defines a geometric region of space
create_box	2 box ->
lattice	fcc 3.61 -> lattice type and lattice parameter
region	cu block 0 50 0 100 0 5 units box -> creates copper atoms in the simulation
box	
create_atoms	1 region cu units box
set	region cu type/fraction 2 0.5 123456
region	vo cylinder z 25 50 5 0 5 units box-> void formation
group	void region vo
delete_atoms	group void
timestep	0.002 -> sets the timestep for subsequent simulations
pair_style	eam/alloy
pair_coeff	* * AlCu.eam.alloy Al Cu → specifies the potential file used

```
#
#minimize      3e-7 3e-8 10000 10000

thermo        10 →computes and prints thermodynamic data after every 10 timesteps
thermo_style   custom step temp vol press etotal

compute       myRDF all rdf 10
fix           11 all ave/time 10 1 10 c_myRDF file cu_melt_new.rdf mode vector

dump          1 all atom 1AlCu_crystal_melt_3d_s_dump_new.lammpstrj .....→dumps a
snapshot of atom quantities every 100 timesteps to the specified file
dump_modify   1 scale no →modifies parameters of previously defined dump command.
A value of scale 'no' means atom coordinates are written in absolute distance units

log logAlCu_crystal_melt_3d_s_new.data

velocity      all create 50 873847 rot yes mom yes dist gaussian

#fixes
fix           1 all npt temp 50 50 0.01 iso 0.0 0.0 0.2 ->fixing the temperature and pressure of the
system
run 1000 ->number of iterations of the simulation
unfix 1
```

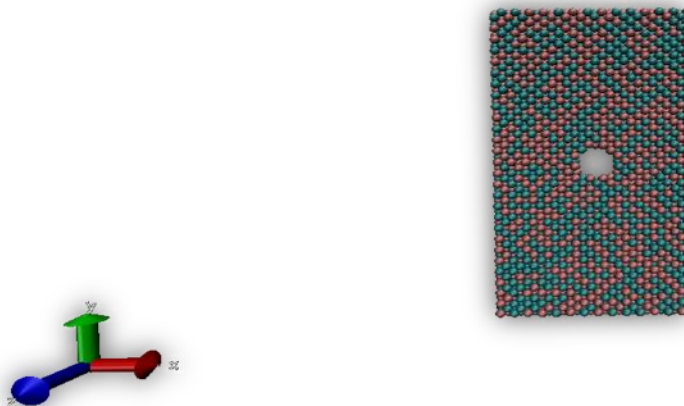


Fig 4.1 Copper-Aluminium alloy crystal having dimensions 100Å x 50Å x 5 Å with a void

4.2 Tensile Deformation of Alloy Specimen:

4.2.1 Computational Steps:

- We need 4 files to run tensile deformation simulation program namely in.file, read_data file, potential file and lammmps.exe file in a single folder.
- b) Read_data file contains the atomic co-ordinates of the atoms of the quenched specimen and this file can be created from the data in last iteration step in dump file obtained after simulation of quenching.
- c) Output files are dump file, dump.stress file, log file, log.lammps file.
- d) Dump file gives the value of Stress and Strain during the loading which will be used to plot Stress Vs Strain curve.

Here the purpose of simulation is to do uniaxial tensile deformation of the specimen along y-direction. Given below is the in.file that contains all the commands required to do simulation of tensile deformation. First the deformation was carried out for different temperatures at a particular strain rate and then the Strain rate was also subsequently varied along with varying the temperature. The whole calculation is performed by large-scale atomic/molecular massively parallel simulator (LAMMPS) [6].

4.2.2 Uniaxial Testing of the specimen

Units	metal
Echo	both
atom_style	atomic
#dimension	2
Boundary	p p p
read_data	AlCu_void.txt -> reads the data file containing the atom positions of the equilibrated crystal in the specified file
timestep	0.002
compute	myrdf all rdf 100
fix	a all ave/time 10 2 100 c_myrdf file W_rdf_nnnd mode vector
compute	1 all stress/atom
compute	2 all reduce sum c_1[1] c_1[2] c_1[3]
variable	stress equal ((c_2[2])/(3*vol))
variable	tmp equal ly
variable	lo equal \${tmp}
variable	strain equal (ly-v_lo)/v_lo
variable	p equal -pyy/10000
thermo	100
thermo_style	custom step temp vol etotal pyy lx ly lz v_stress v_strain

```

pair_style      eam/alloy
pair_coeff      * * AlCu.eam.alloy Al Cu

dump           1 all custom 100 NVT_defo_nnndump_Cu-void.lammpstrj id type x y z

log            NVTlogdef_nnn_cu_void.data

velocity       all create 400 873847 rot yes mom yes dist gaussian

```

tensile deformation

```

fix            2 all deform 1 x volume y erate 0.1 z volume units box ->strain rate of
0.1 sec-1 is applied in y direction

```

temperature controller

```

fix            1 all nvt temp 400 400 0.1 ->fixing the temp of system
fix            def all print 1 "${strain} ${p}" file Cu_nnn_100.def1NVT.txt
run            1000->Number of iterations of the simulation

```

4.3 Simulation results

4.4 Tensile testing at 10^{11} s⁻¹ strain rate for different temperatures

Simulation was carried out at 10^{11} /s strain rate and at different temperatures (50K, 300K, 400K) and the test data were plotted in the form of Stress- Strain curves. Given below is the Stress -Strain curve at different temperatures.

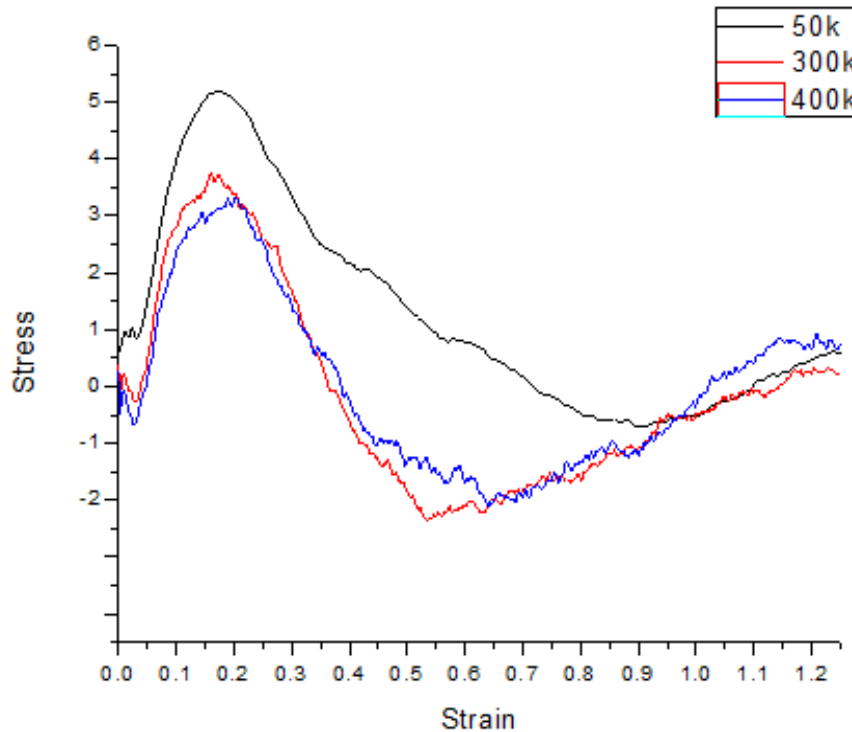


Fig 4.2 Stress Strain curve for Cu₅₀Al₅₀ Alloy at 10^{11} Strain rate and at different temperatures (50K, 300K, 400K)

4.4.1 Comparison of uniaxial-tensile properties of the specimen at different temperatures

Deformation temp.	Ultimate tensile strength	Fracture Stress
50K	5.10 GPa	0.71 GPa
300K	3.56 GPa	0.71 GPa
400K	3.20 GPa	0.58 GPa

This is well understood that strength of metallic materials decreases with increasing temperature [8,14]. From the simulation results on nanoscale copper and aluminium alloy, similar results have been obtained. The stress-strain curves at 50 K, 300 K and 400 K when plotted in a single graph clearly indicates the effect of temperature as illustrated in Figures above. It can be seen from the figure above that on increasing the temperature, the stress-strain curves dropped down, as expected. They show a decrease in the ultimate tensile stress with decreasing load rate as supported by both theory and experimentation [13].

4.4.2 Nature of the curve explained by VMD snapshots

(a) First peak is obtained when the behavior of the deformation changes from elastic to plastic of the $\text{Cu}_{50}\text{Al}_{50}$ crystal and then then stress value begins to decrease. This fact is well supported by the VMD snapshot, which is presented below. The below VMD snapshots are obtained for just before the peak of the curve, at the peak and when the stress value is just starting to decreasing. VMD snapshots clearly show the formation of micro voids when a strain above a particular value is reached, i.e. when the sample enters into plastic region from elastic one.

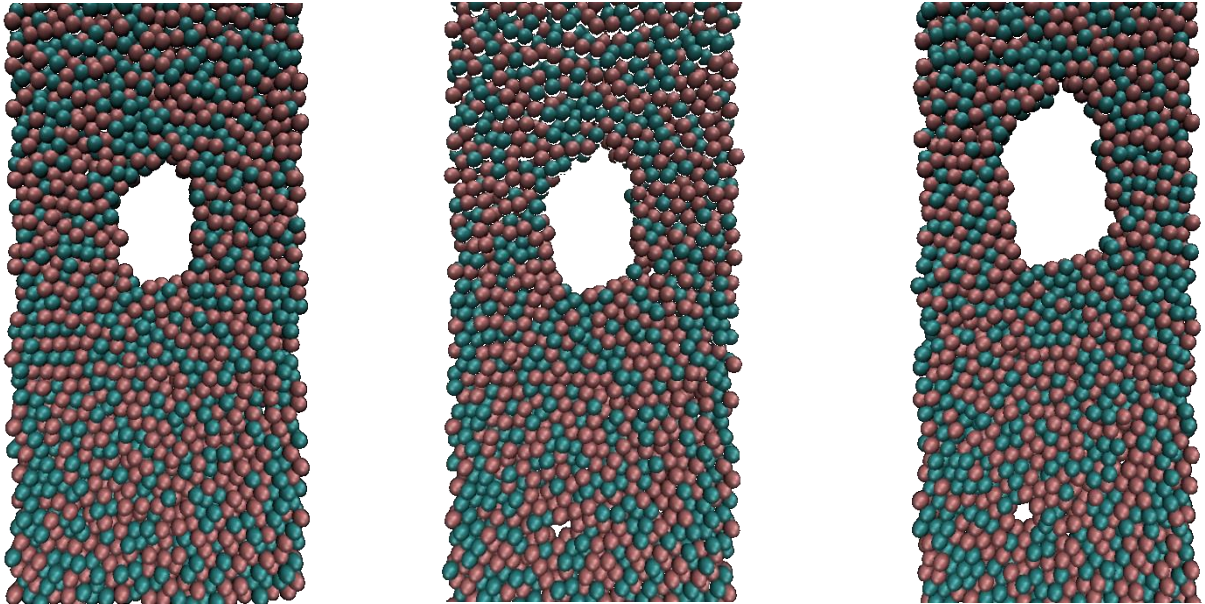


Fig 4.3 VMD snapshots of the specimen when deformed in elastic region at strain rate of 0.1 ps^{-1} applied in y direction

(b)After reaching a minima the stress value again starts to increase due to the closure of the voids initially formed and due to significant rearrangement of the BCC structure into a new one .As it can be easily seen in the VMD snapshots.

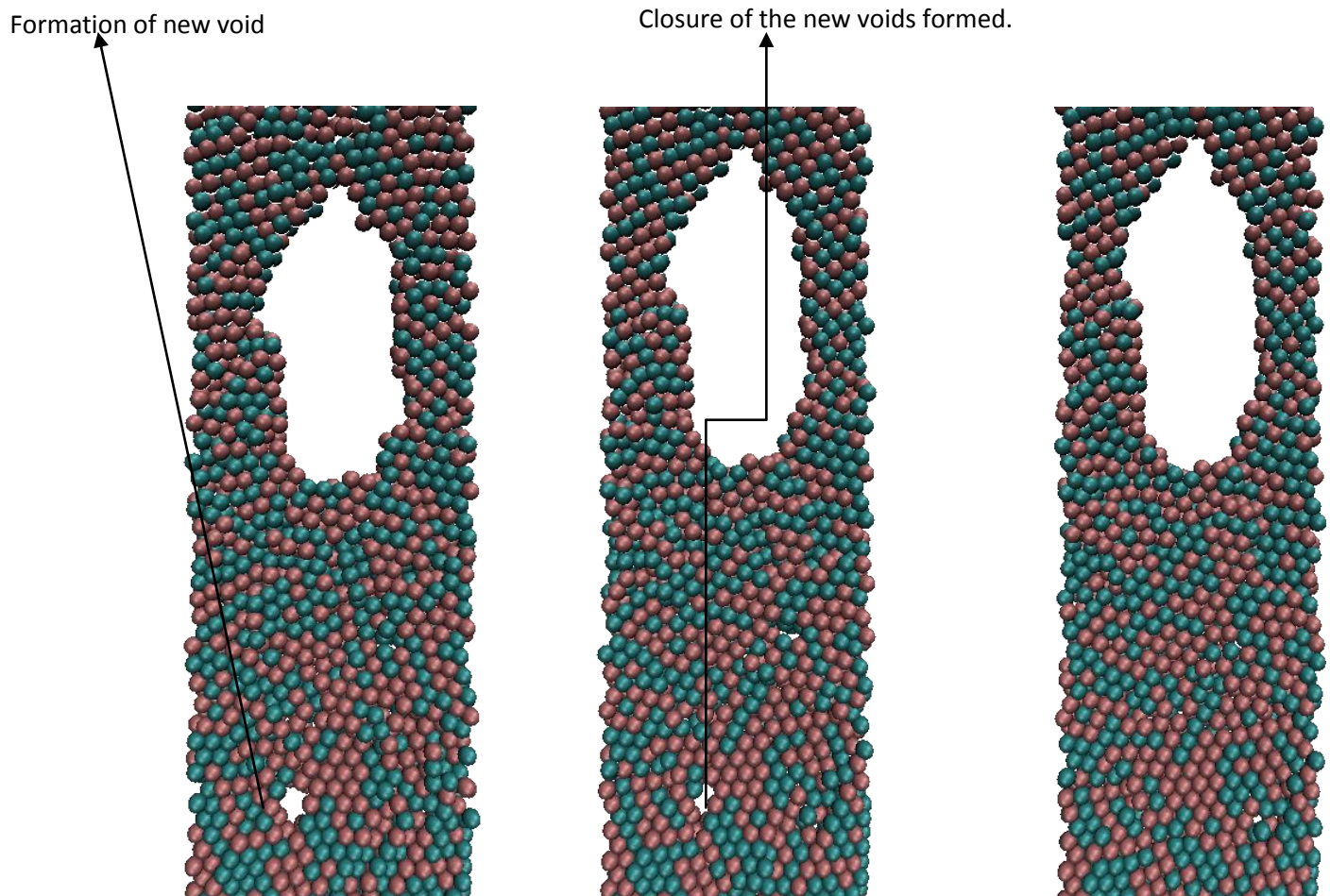


Fig 4.4 VMD snapshots of the specimen at different strain values

The stress value after that increases for a very short duration of time when the specimen thins so much that on further application of load the specimen is unable to bear the load and it fractures from middle which can be seen in the VMD snapshots very clearly.

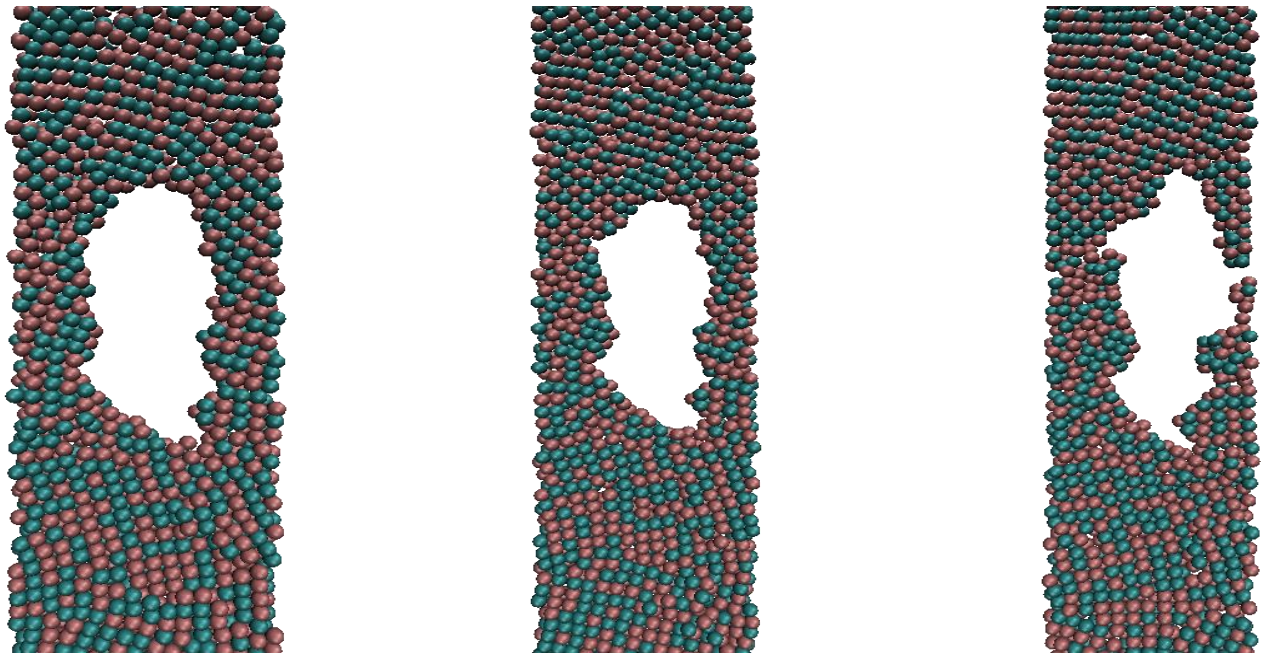


Fig 4.5 VMD snapshots of the specimen at the time of getting fractured

At 300 and 400K failure occurs in a similar fashion as also indicated by the tensile curve .The only difference being that the failure occurs at a lower stress level than in case of 50K.VMDsnapshots depicting the failure of $\text{Cu}_{50}\text{Al}_{50}$ alloy is shown below at 300K and 400K.

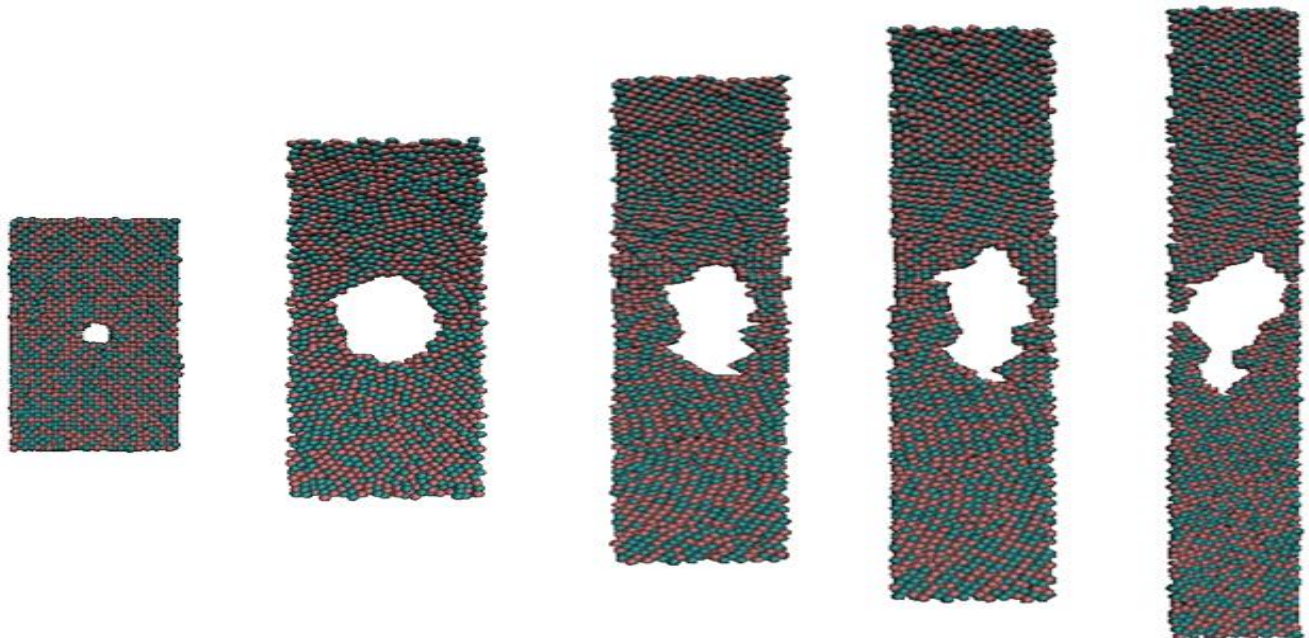


Fig 4.6 VMD snapshots depicting failure of the $\text{Cu}_{50}\text{Al}_{50}$ alloy at different timesteps (2000, 4000, 6000, 8000, 10000) when tensile testing is carried out at 300K

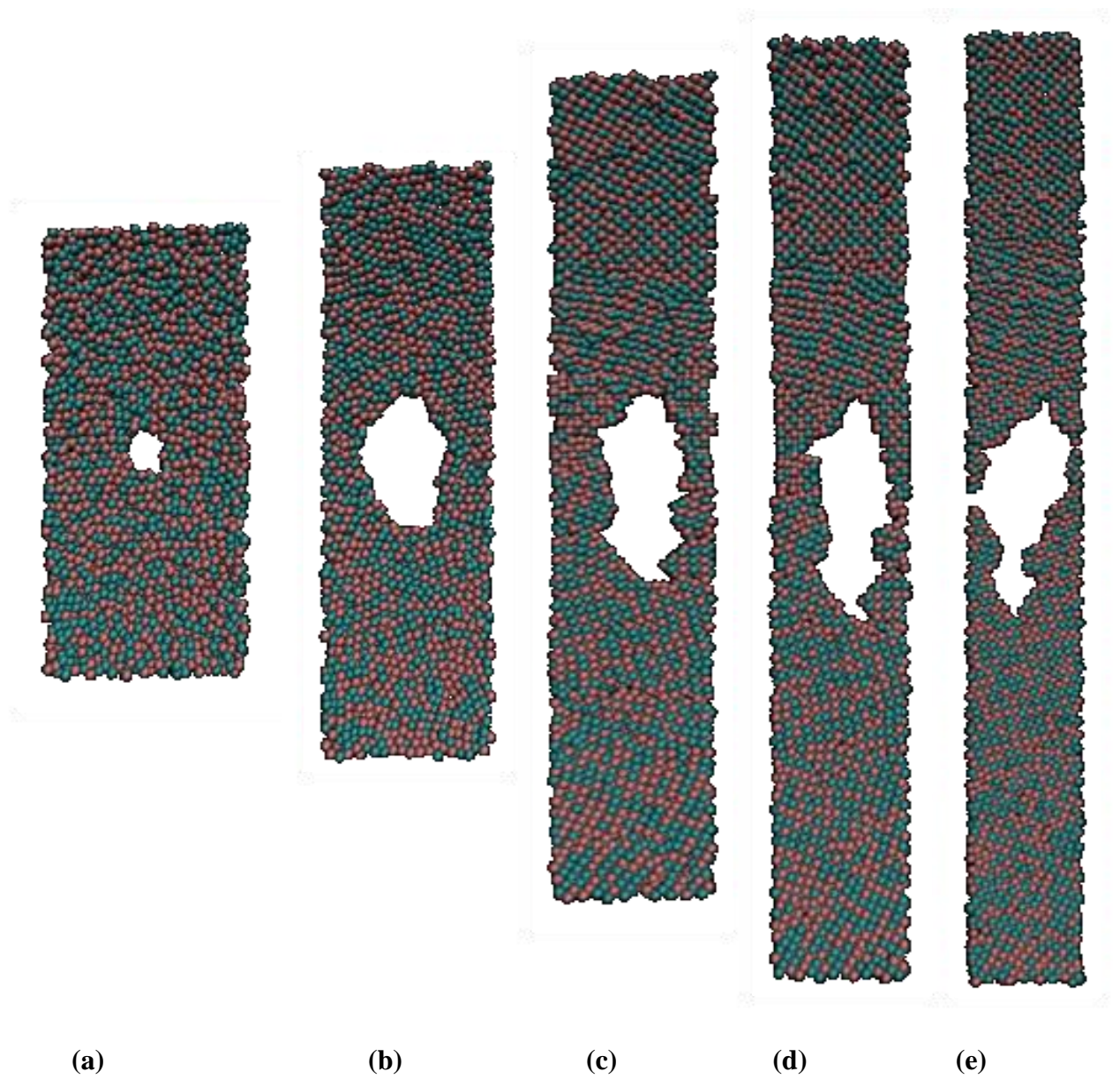


Fig 4.7 VMD snapshots depicting failure of the $\text{Cu}_{50}\text{Al}_{50}$ alloy at different timesteps (2000,4000,6000,8000,100000) when tensile testing is carried out at 500K

4.5 Tensile testing $5 \times 10^{11} \text{ s}^{-1}$ strain rate for different temperatures

Simulation was carried out at $5 \times 10^{11} \text{ s}^{-1}$ strain rate and at different temperatures (50K, 300K, 400K) and the test data were plotted in the form of Stress- Strain curves. Given below is the Stress -Strain curve at different temperatures.

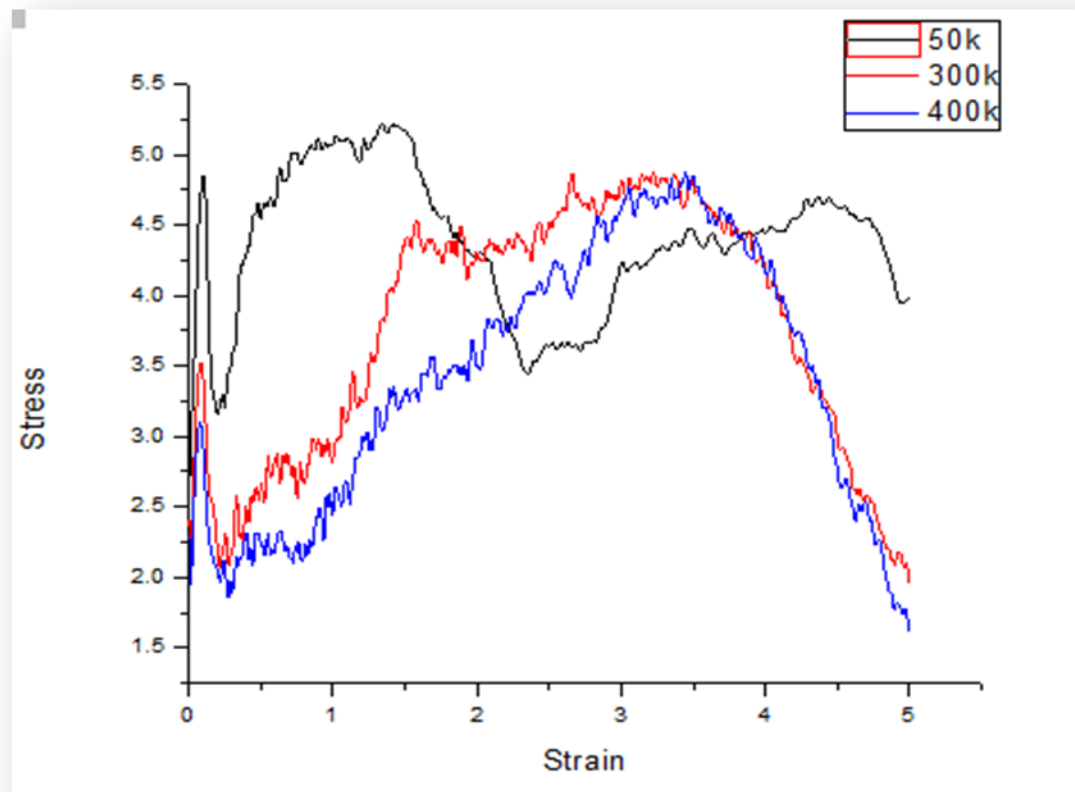


Fig 4.8 Stress Strain curve for $\text{Cu}_{50}\text{Al}_{50}$ Alloy at 5×10^{11} Strain rate and at different temperatures (50K, 300K, 400K)

5 4.5.1 Comparison of Tensile properties of the specimen at different temperatures

Deformation temp.	Ultimate tensile strength	Fracture Stress
50K	5.25GPa	3.96 GPa
300K	4.75 GPa	2.07 GPa
400K	4.55 GPa	1.69 GPa

4.5.2 Nature of the curve explained by VMD snapshots

The behavior of the curve is somewhat similar to that obtained in case of tensile deformation at 50K with the only difference is a series of steps of rise and fall of the stress values in the initial elastic region, which is then followed by a plastic region up to a maximum stress. This behavior can be attributed to strain hardening and subsequent softening of the material due to dislocation pileup and subsequent rapid movement due to the generations of the dislocations [10]. Animation of the tensile tests indicated considerable reorganization of the atoms followed by rapid movement due to the generation of dislocations [10].

In this case also failure occurs by formation of voids there coalescence into nano-cracks and subsequent failure or rupture of the specimen, which can be shown with the help of the VMD snapshots.

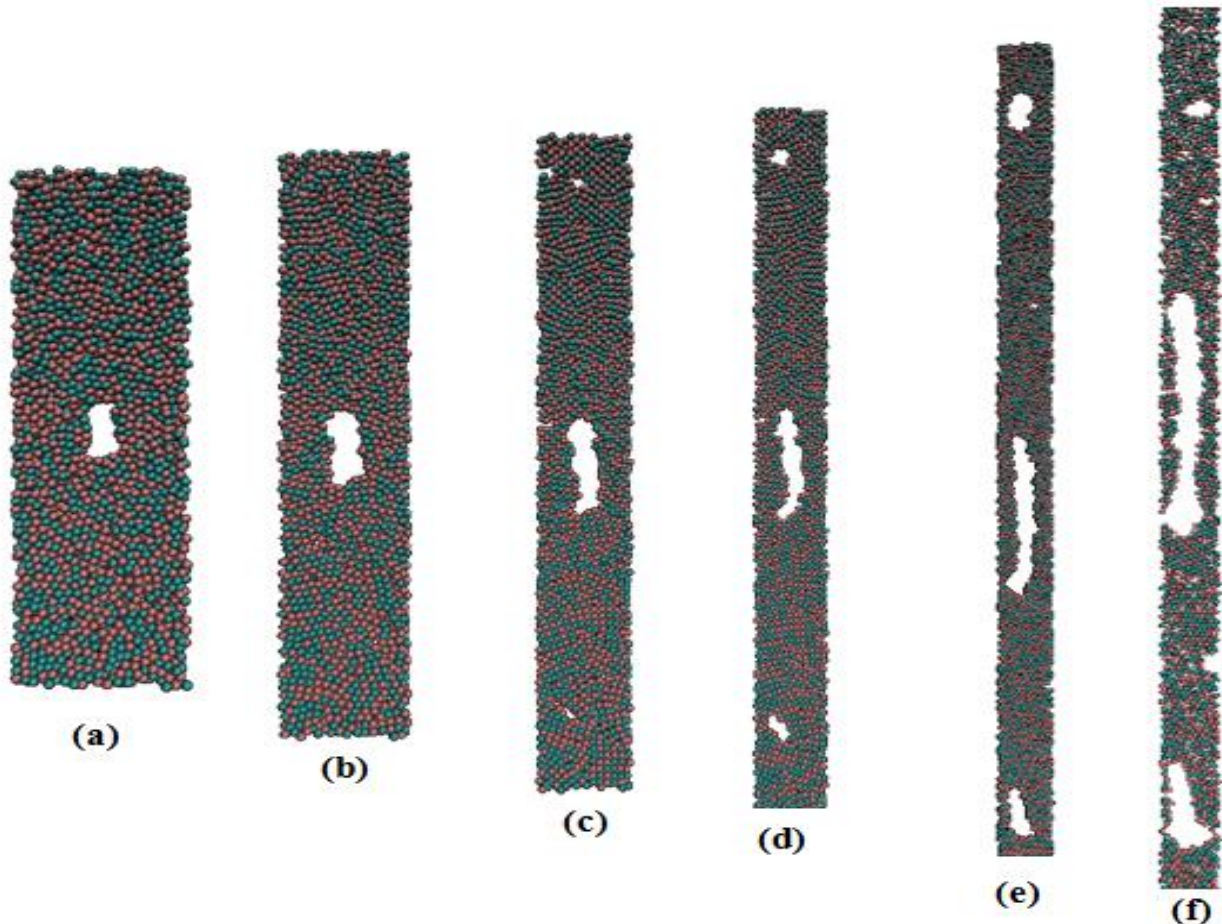


Fig 4.9 VMD snapshots depicting failure of the $\text{Cu}_{50}\text{Al}_{50}$ alloy when tensile testing is carried out at 50K (a)900; (b)1500; (c)2800; (d)3500; (e)4300; (f) 5000 timesteps

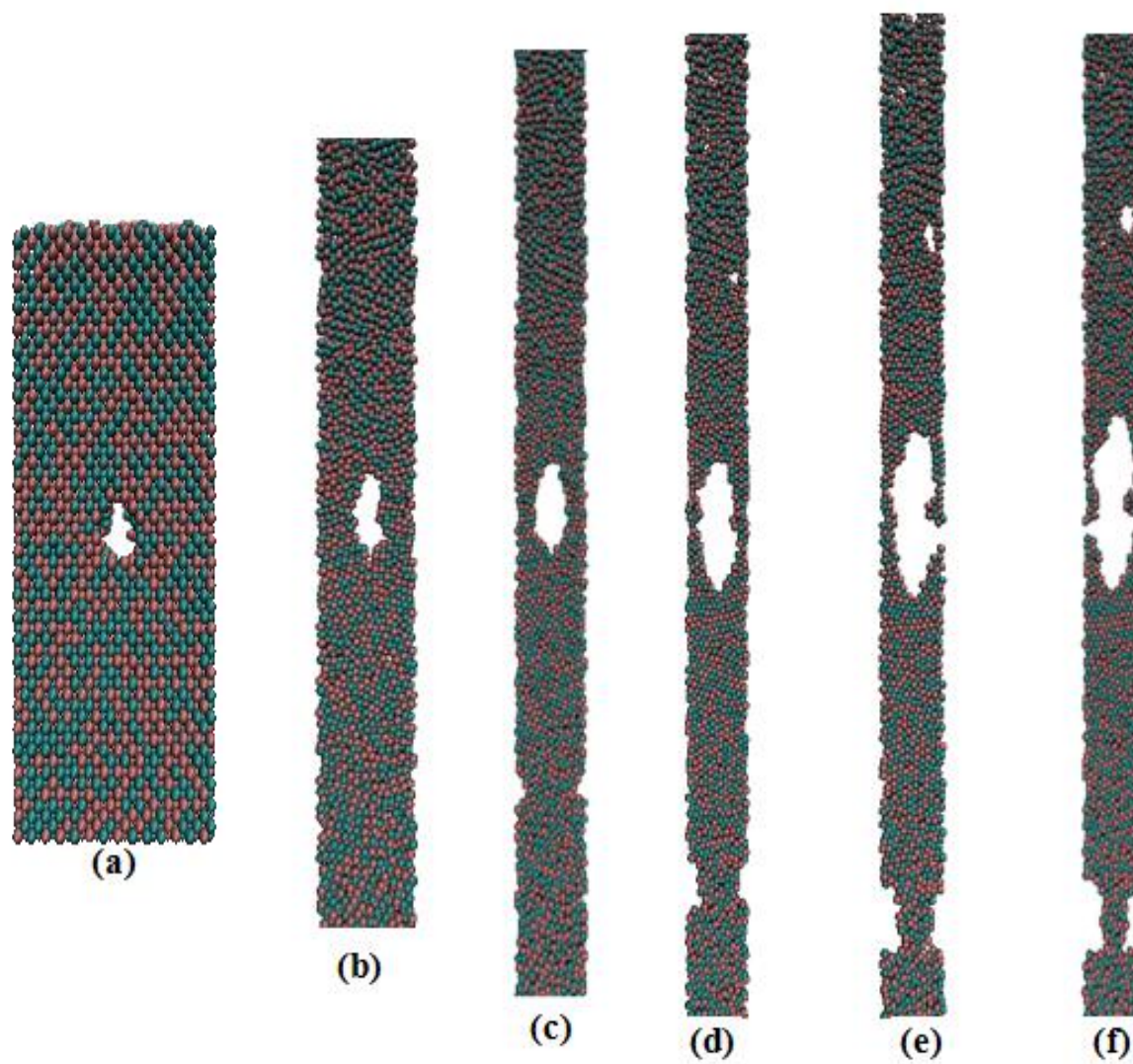


Fig 4.10 VMD snapshots depicting failure of the Cu₅₀Al₅₀ alloy when tensile testing is carried out at 50K (a)900; (b)1500; (c)2800; (d)3500; (e)4300; (f) 5000 timesteps

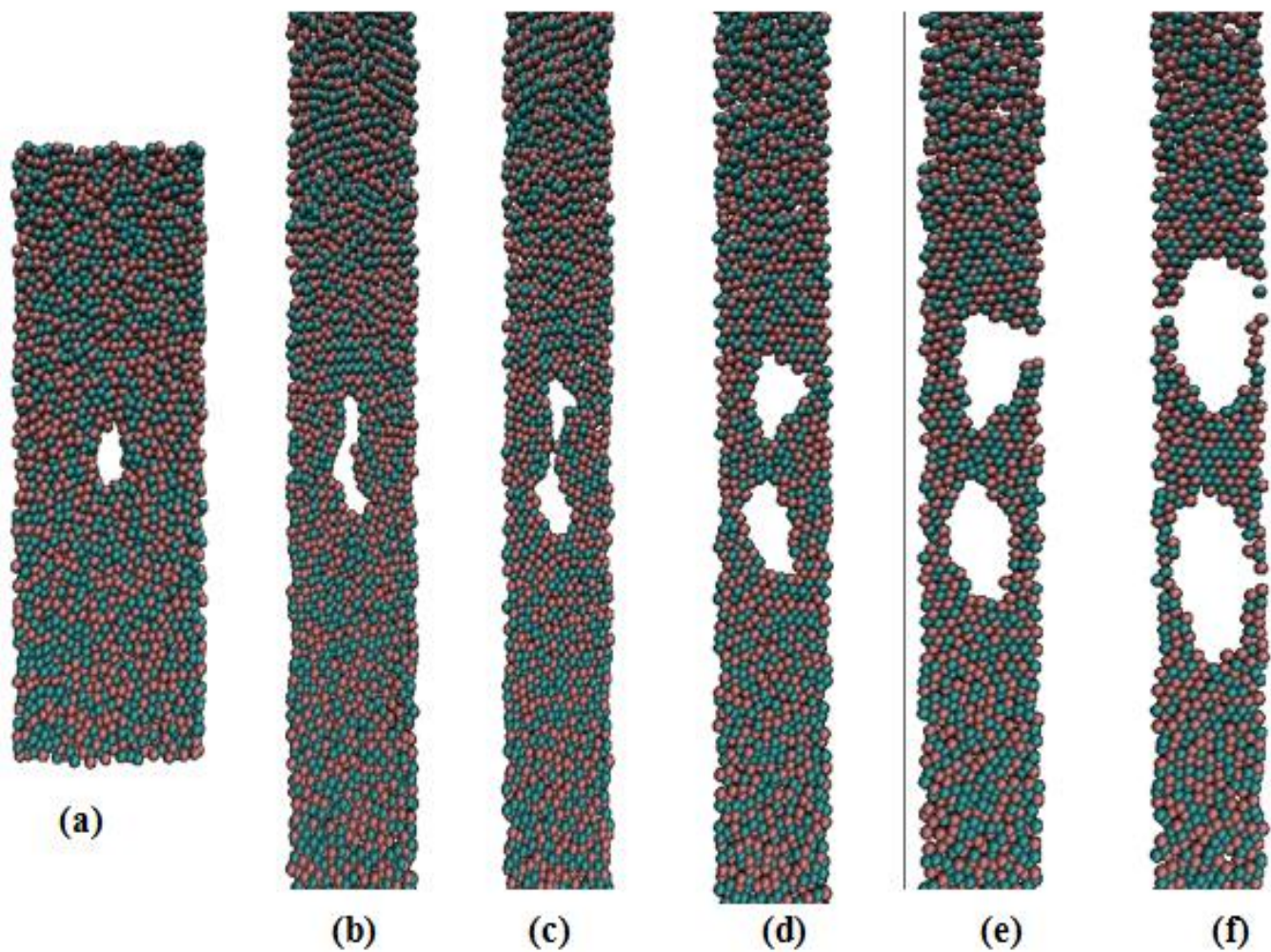


Fig 4.11 VMD snapshots depicting failure of the $\text{Cu}_{50}\text{Al}_{50}$ alloy when tensile testing is carried out at 50K (a)900; (b)1500; (c)2800; (d)3500; (e)4300; (f) 5000 timesteps

Very peculiar behavior can be seen in this case the void which was initially present elongated in the direction of application of load .As the test is continued by constantly applying increasing load void which was initially present got spited into two due to atomic rearrangement and then necking started at those two voids which ultimately lead to the failure of the specimen.

4.6 Effect of varying temperature at 10^{12} strain rate

Simulation was carried out at 10^{12} /s strain rate and at different temperatures (50K,300K,400K) and the test data were plotted in the form of Stress- Strain curves. Given below is the Stress - Strain curve at different temperatures.

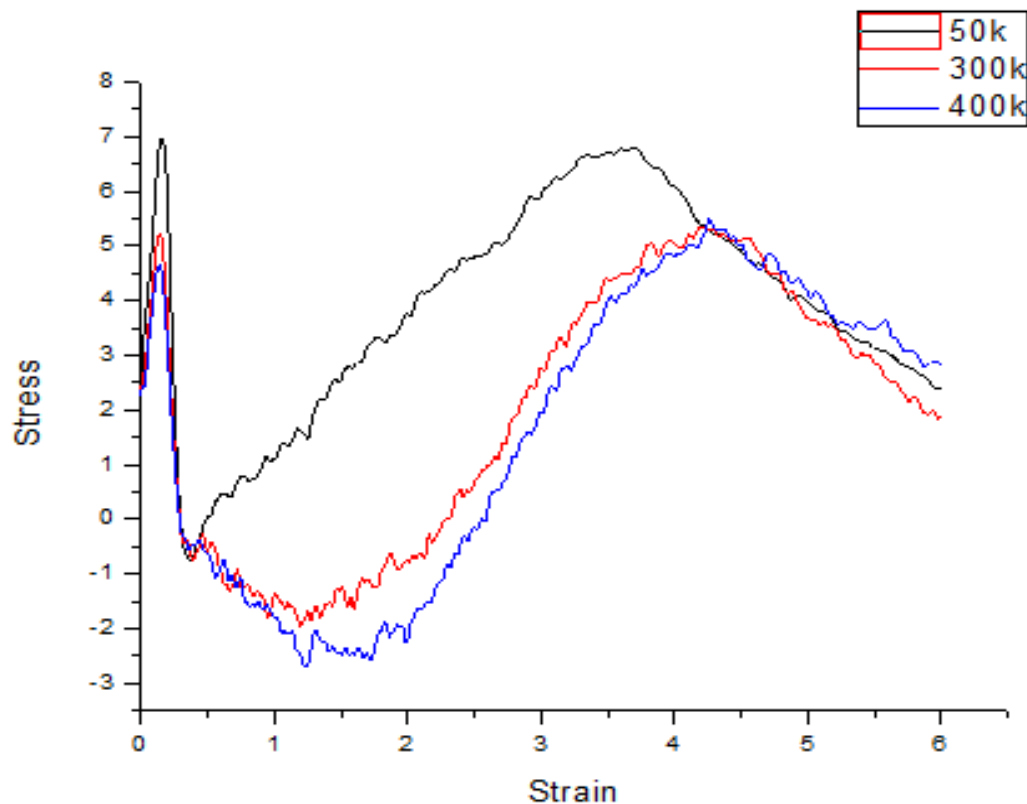


Fig 4.12 Stress Strain curve for Cu₅₀Al₅₀ Alloy at 10^{12} Strain rate and at different temperatures (50K, 300K, 400K)

4.6.1 Comparison of Tensile properties of the specimen at different temperatures

Deformation temp.	Ultimate tensile strength	Fracture Stress
50K	6.94 GPa	2.83 GPa
300K	5.16 GPa	2.43 GPa
400K	4.63 GPa	2.03 GPa

The decrease in the ultimate tensile strength in accordance to the fact that at higher temperatures the strength of the material decreases which is also observed when experiments are carried out at macro scale level.

4.6.2 Nature of the curve explained by VMD snapshots

1. The stress value becomes negative after certain strain value. This may be due to the fact that atoms in BCC lattice rearrange themselves to form a new crystal structure during loading because of which the new structure formed is slightly under compression because of the internal forces present in the new structure which causes the forces to drop to a negative value[10]. The rearrangement in the microstructure can be easily shown in the VMD snapshots.

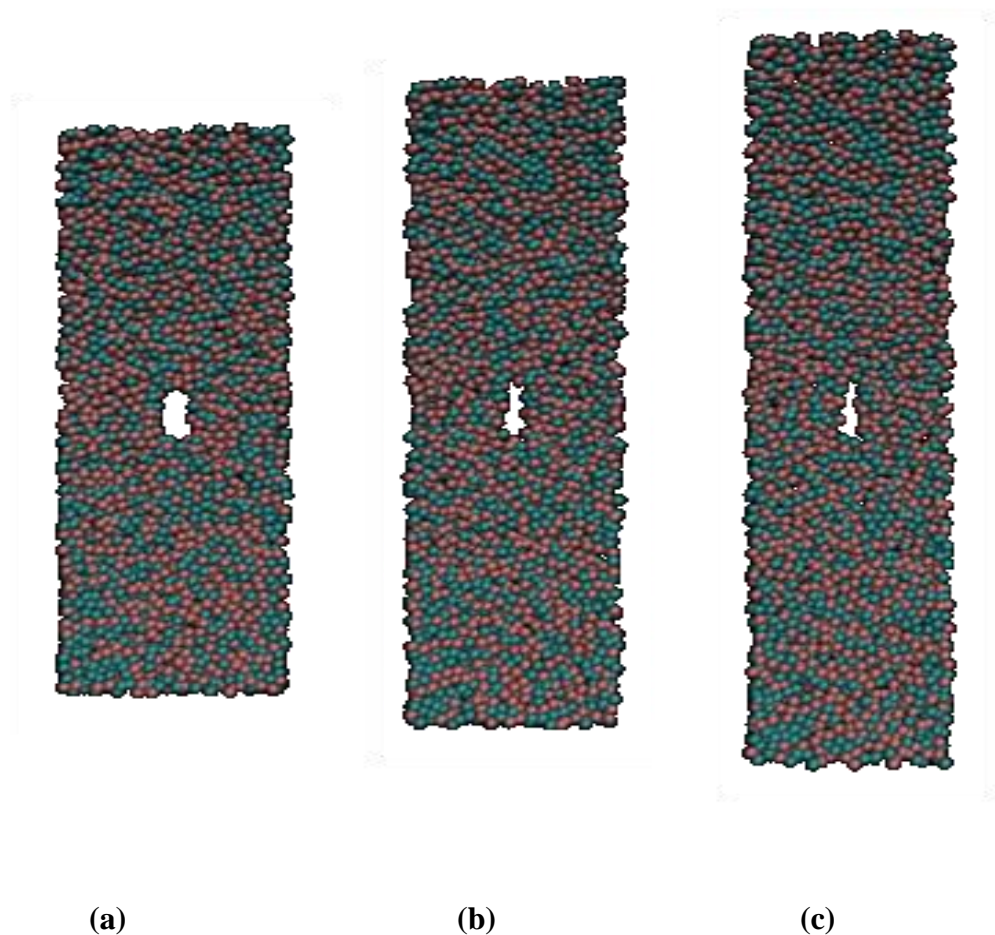


Fig 4.13 VMD Snapshots of the rearrangement of atoms to form new crystal structure during tensile testing resulting in near closure of the voids

Failure occurs in the specimen in a manner similar to what is observed at macro scale i.e. due to void formation their subsequent coalescence to form nano cracks and subsequent fracture or separation as shown in the VMD snapshots.

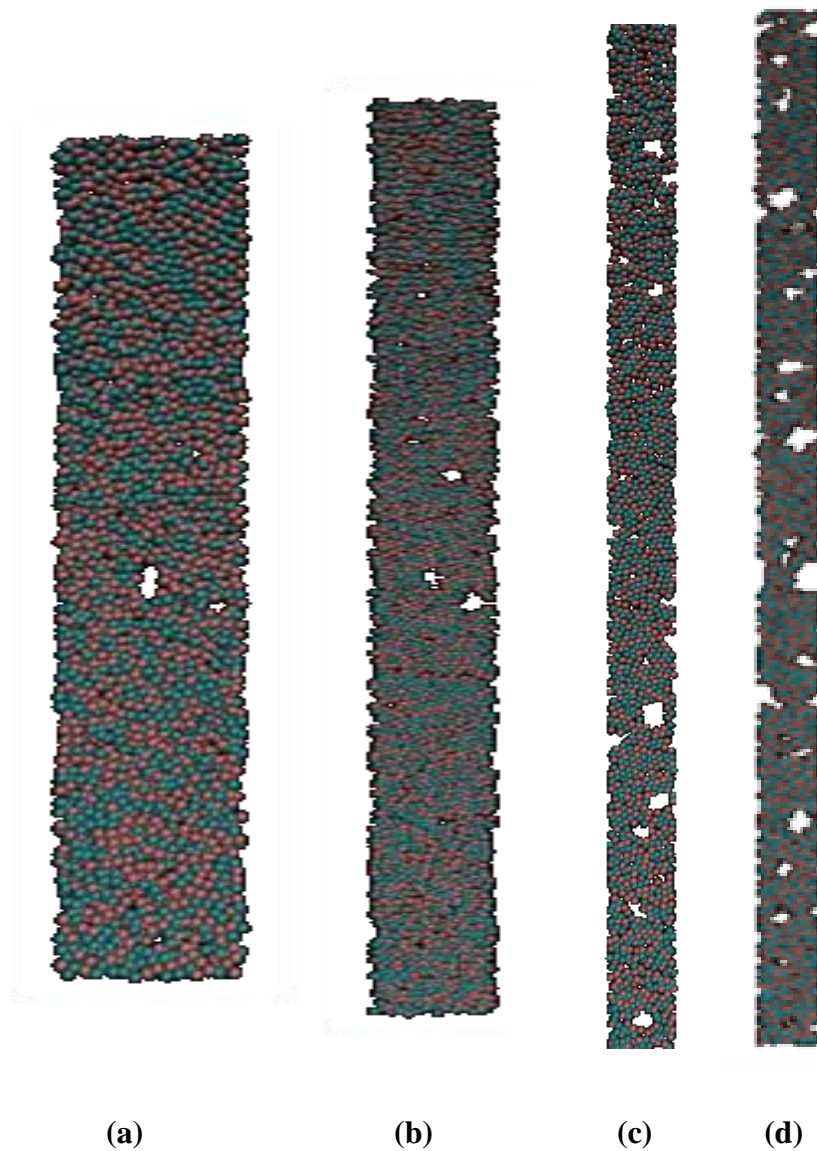


Fig 4.14 VMD snapshots showing the failure of the specimen via formation of new voids and their coalescence to form nano cracks

Fracture takes place in a similar manner in case when the samples are tested at higher temperatures ie 300K and 400K the only difference being that the fracture takes place subsequently lower stresses at higher temperature because of decrease in strength which is in accordance to what is observed at macro level failure

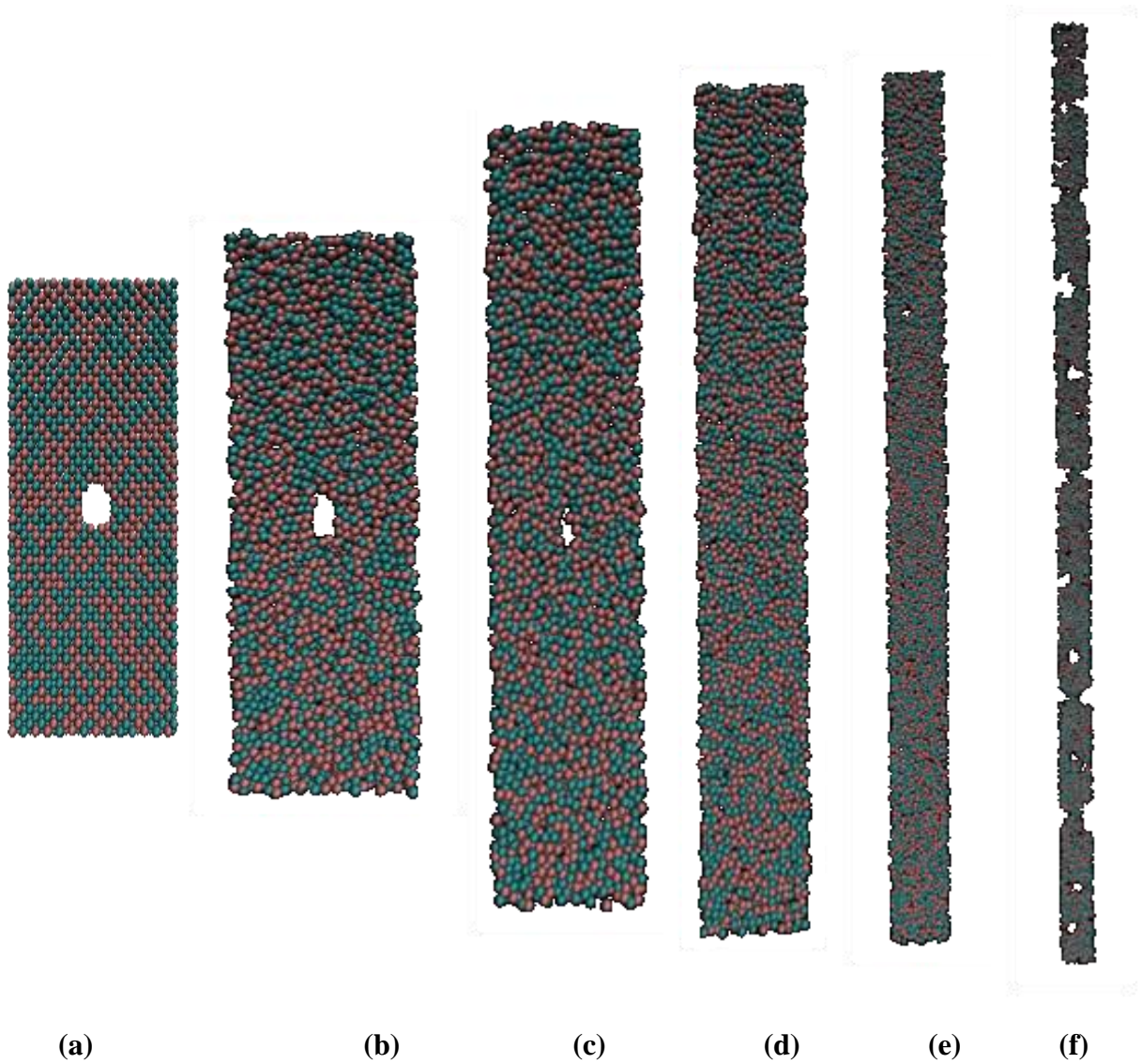


Fig 4.1 VMD snapshot showing failure of Cu₅₀Al₅₀ alloy when tested at 10^{12} s^{-1} strain rate for 300K at (a)100,(b)1000,(c)1500,(d)2000,(e)2500,(f)3000 timesteps

It can be clearly seen from the (a),(b) and (c) crystal structure that significant amount of crystal rearrangement takes place which even results in the closure of the void initially present. Subsequently voids get formed in the later stages of the test. If the tests are continued after that then coalescence of these voids into nano cracks leads to fracture of the specimen as shown in the snapshots (d) and (e).

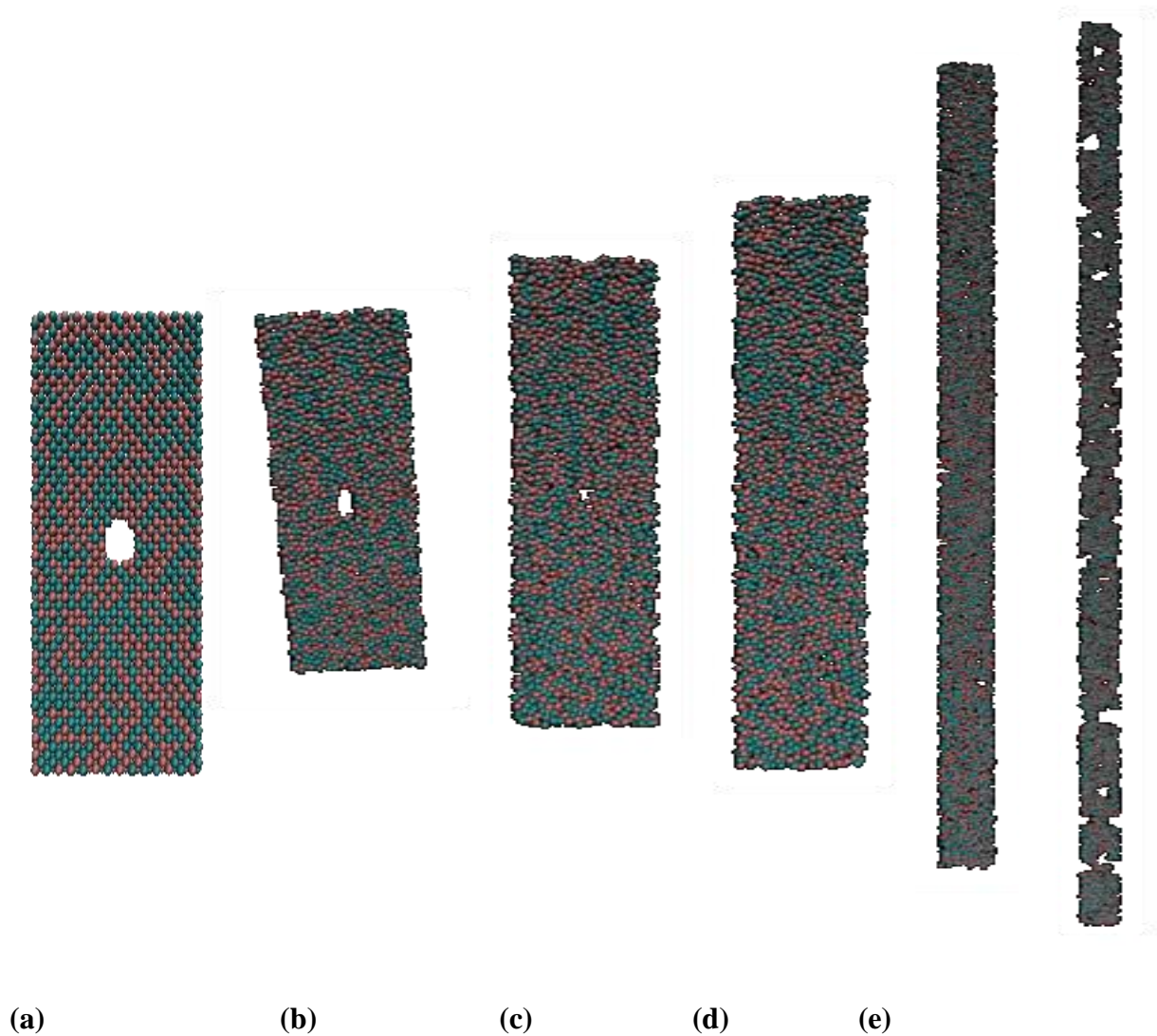


Fig 4.16 VMD snapshot showing failure of Cu₅₀Al₅₀ alloy when tested at 10¹² s⁻¹ strain rate at 400K (a)100,(b)1000,(c)1500,(d)2000,(e)2500,(f)3000 timesteps

Exactly similar failure mechanism is seen in this case also than what was seen for tensile deformation at 50K and 300K.

5. Biaxial tensile testing of Cu₅₀Al₅₀ alloy at different strain rates

After the uniaxial testing of the specimen at different strain rates as well as at different temperatures biaxial tensile testing of the specimen was carried out at 300K for different strain rates.(10^{11} , 5×10^{11} and 10^{12}) by applying force in the Y direction along with X direction. The tests were not carried out at different temperatures because we already have seen that on increasing the temperature strength of the materials decreases but the overall mechanism for failure remains the same. The stress strain values obtained is plotted on a single graph so as to compare the values of UTS and fracture stress at different strain rates

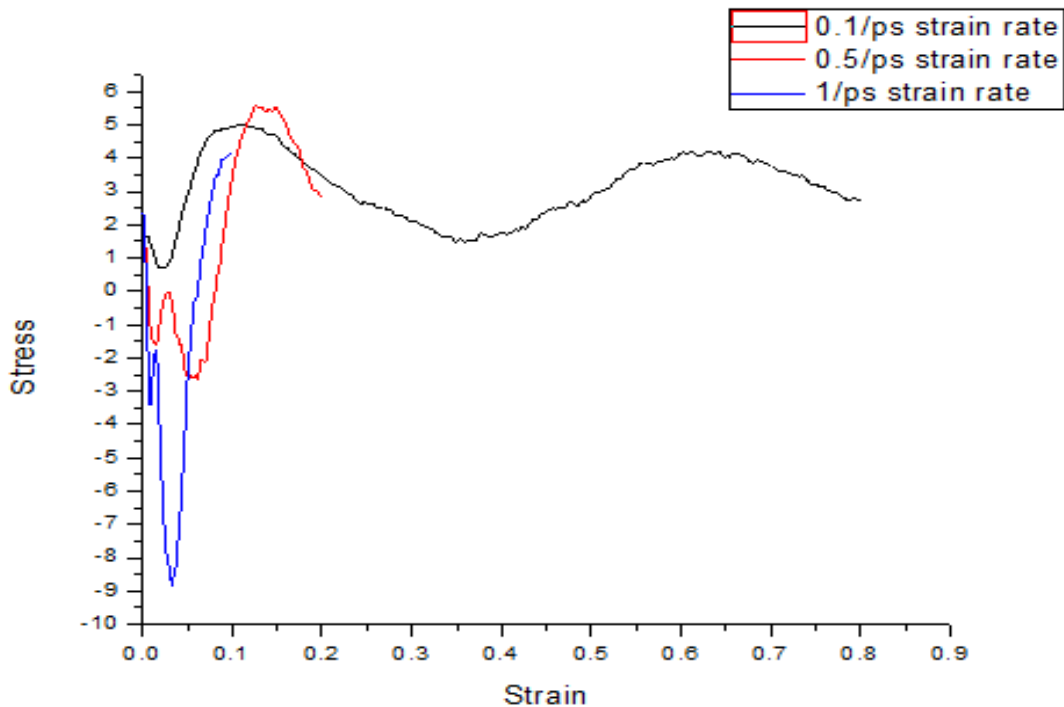


Fig 5.1 Stress Strain curve for various strain rates under biaxial loading

5.1 Comparison of tensile properties obtained for different rate of loading

Strain Rate	Ultimate tensile strength	Fracture Stress
10^{11} /s	5.51GPa	2.88GPa
5×10^{11} /s	4.97GPa	4.97Gpa
10^{12} /s	4.01Gpa	2.70Gpa

On comparing the tensile values obtained we observe that no definite pattern can be found for flow stress with increasing strain rate, also the failure mechanism observed in case of biaxial testing is quite complex unlike in case of uniaxial testing where failure occurred due to necking and subsequent failure of a localized region. In case of biaxial tensile testing localized deformation is not observed instead plastic deformation occurs at various points in the specimen. Thus the specimen does not get fractured at a specific point but at various points as it can be clearly shown by the VMD snapshots given below.

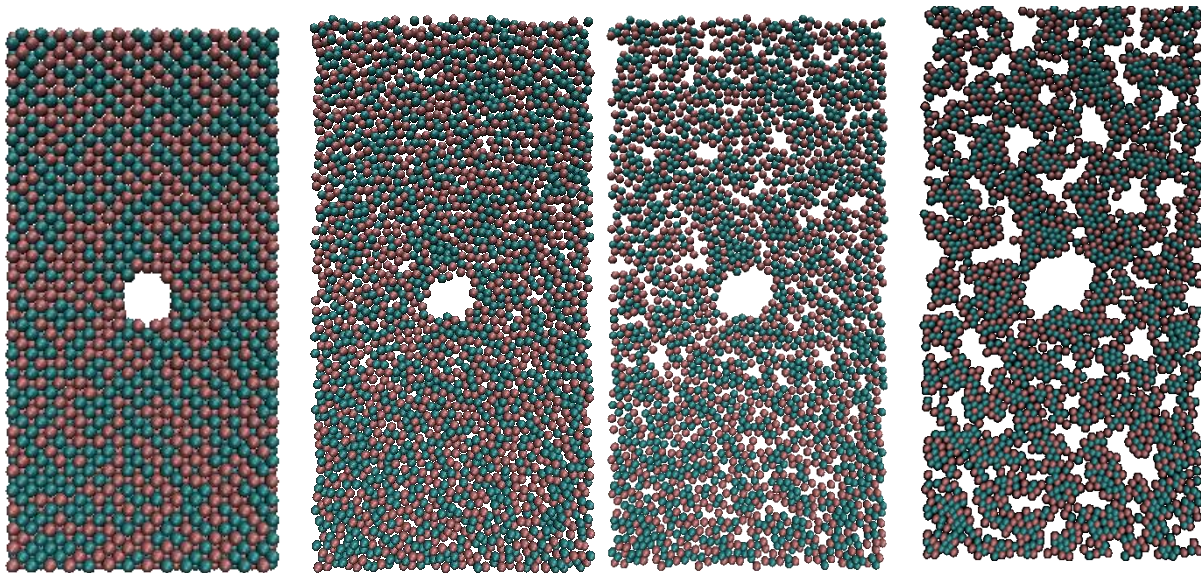


Fig 5.2 VMD snapshot showing the failure of the specimen for 10^{11} strain rate at 300K [500,2000,3000,4000 timesteps]

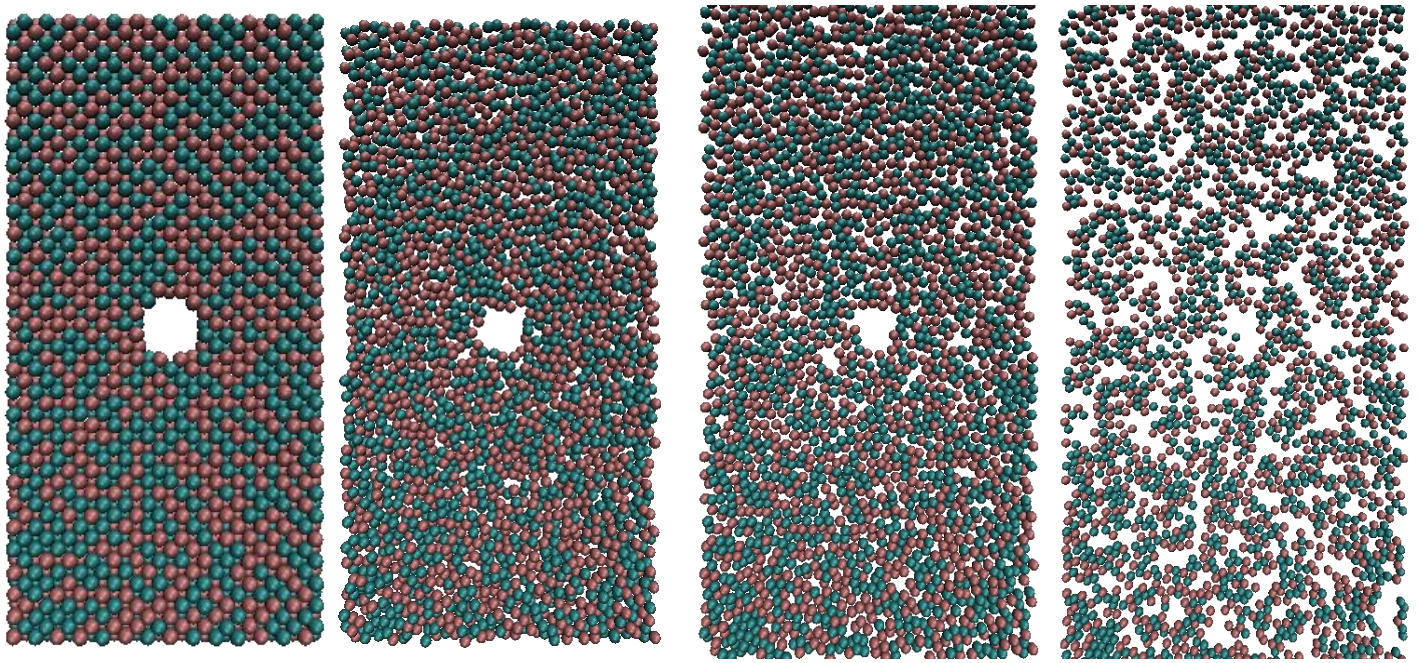


Fig 5.3VMD snapshot showing the failure of the specimen at 5×10^{11} strain rate at 300K[500,2000,3000,4000 timesteps]

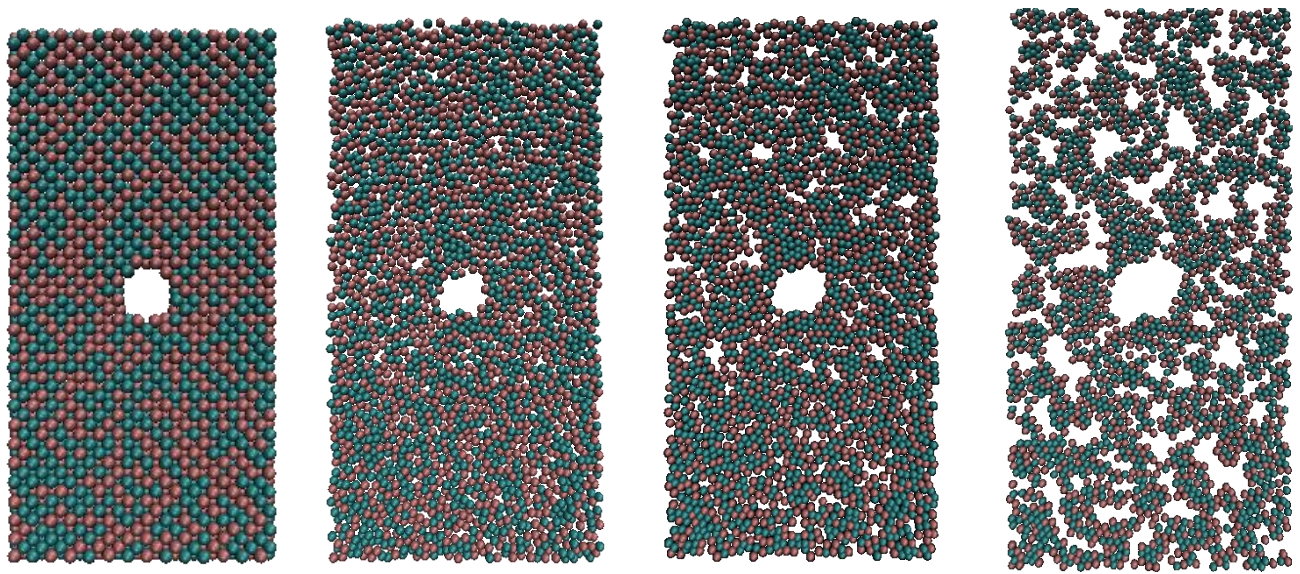


Fig 5.4VMD snapshots showing the failure of the specimen for 10^{12} strain rate at 300K [500,2 000,3000,4000 timesteps]

6. Conclusions

Based on the tensile tests carried out various strain rates and temperatures on the Cu₅₀Al₅₀ alloy crystalline model the following conclusions can be listed.

1. MD simulation was done and failure mechanism in uniaxial mode was studied and it was found out that the fracture of the specimen occurs via void formation, their coalescence to form cracks which ultimately leads to failure.
2. In conventional tensile testing, a linear stress-strain graph is obtained in linear region, in case of nano-tensile testing, a number of sudden ups and downs is observed in the initial elastic region which is then followed by a plastic region. These fluctuations are a result of the rapid strain hardening and subsequent softening of the specimen.
3. The deformation under biaxial mode is quite complex as necking is not observed and the sample fractured by coalescence of several nano-voids leading to fracture.

7. References:-

- [1] <http://www.emeraldinsight.com/journals.htm?articleid=1686858&show=abstract>
- [2] http://www.copper.org/resources/properties/microstructure/al_bronzes.html
- [3] Lin Yang, R. Hood, R. Rudd, B. Lee, & John Moriarty. Atomistic Simulation: Molecular Statics and Molecular Dynamics (https://www-pls.llnl.gov/?url=about_pls-condensed_matter_and_materials_divisioneos_materials_theory-methods-md)
- [4] KOTRECHKO S A, FILATOV A V, OVSIANNIKOV A V. Molecular dynamics simulation of deformation and failure of nanocrystals of bcc metals [J]. Theoretical and Applied Fracture Mechanics, 2006, 45: 92–99.
- [5] <http://www.wikipedia.com>
- [6] S. Plimpton, Fast Parallel Algorithms for Short-Range Molecular Dynamics, [J]. Comp Phys, 117, 1-19 (1995) (<http://lammps.sandia.gov>)
- [7] Satyanarayan Dhal, Yadlapalli Raja, Effect of size and strain rate on deformation behaviour of Cu₅₀Zr₅₀ metallic glass: A molecular Dynamics Simulation study. B.Tech thesis. NIT Rourkela
- [8] G. E. Dieter, Mechanical Metallurgy, London, Mc-Graw Hill Publication (1988).
- [9] William Humphrey, Andrew Dalke, Klaus Schulten, VMD: Visual Molecular Dynamics, Journal of Molecular graphics 14;33-38, 1996
- [10] R. Komanduri, N. Chandrasekaran, L.M. Raff .Molecular dynamics (MD) simulation of uniaxial tension of some single-crystal cubic metals at nanolevel [J]. Mechanical Sciences 1-24 (2001)
- [11] Lin Yuan and Debin Shan, Bin Guo Molecular dynamics simulation of tensile deformation of nano- single crystal aluminium [J]. Materials Processing Technology ,2006)
- [12] ZENG Xiang-guo, XU Shu-sheng, CHEN Hua-yan, LI Ji-liang. Molecular dynamics simulation on plasticity deformation mechanism and failure near void for magnesium alloy

- [13] R.W. Hertzberg, Deformation and fracture mechanics of engineering materials, New York, John Wiley & Sons, Inc. (1989).
- [14] R.W. Hertzberg, Deformation and fracture mechanics of engineering materials, New York, John Wiley & Sons, Inc. (1989).

